TECHNICAL REPORT
NATICK/TR-13/016

AD ______________

DESIGN OF A HELMET LINER FOR IMPROVED LOW VELOCITY IMPACT PROTECTION

by
John Fitek
and
Erin Meyer

May 2013

Final Report
January 2012 – October 2012

Approved for public release; distribution is unlimited

U.S. Army Natick Soldier Research, Development and Engineering Center
Natick, Massachusetts 01760-5020

DISCLAIMERS

The findings contained in this report are not to be construed as an official Department of the Army position unless so designated by other authorized documents.

Citation of trade names in this report does not constitute an official endorsement or approval of the use of such items.

DESTRUCTION NOTICE

For Classified Documents:

Follow the procedures in DoD 5200.22-M, Industrial Security Manual, Section II-19 or DoD 5200.1-R, Information Security Program Regulation, Chapter IX.

For Unclassified/Limited Distribution Documents:

Destroy by any method that prevents disclosure of contents or reconstruction of the document.

REPORT DOCUMENTATION PAGE				*Form Approved* *OMB No. 0704-0188*

1. REPORT DATE *(DD-MM-YYYY)*	**2. REPORT TYPE**	**3. DATES COVERED** *(From - To)*
08-05-2013	Final	January 2012 – October 2012

4. TITLE AND SUBTITLE	
DESIGN OF A HELMET LINER FOR IMPROVED LOW VELOCITY IMPACT PROTECTION	**5a. CONTRACT NUMBER**
	5b. GRANT NUMBER
	5c. PROGRAM ELEMENT NUMBER
6. AUTHOR(S) John Fitek and Erin Meyer	**5d. PROJECT NUMBER** H98
	5e. TASK NUMBER
	5f. WORK UNIT NUMBER
7. PERFORMING ORGANIZATION NAME(S) AND ADDRESS(ES) U.S. Army Natick Soldier Research, Development and Engineering Center ATTN: RDNS-WSC-M Kansas St.. Natick. MA 01760-5020	**8. PERFORMING ORGANIZATION REPORT NUMBER** NATICK/TR-13/016
9. SPONSORING / MONITORING AGENCY NAME(S) AND ADDRESS(ES)	**10. SPONSOR/MONITOR'S ACRONYM(S)**
	11. SPONSOR/MONITOR'S REPORT NUMBER(S)

12. DISTRIBUTION / AVAILABILITY STATEMENT

Approved for public release; distribution is unlimited

13. SUPPLEMENTARY NOTES

14. ABSTRACT

This report documents a 2012 Natick Soldier Research, Development and Engineering Center (NSRDEC) study that used material testing and modeling tools to design and test a helmet liner prototype for increased low velocity impact protection. Basic theory of energy absorption and packaging were used to estimate material requirements for the helmet application. Foam materials were tested with an impact test device and characterized based on foam compression strength and energy absorbing efficiency. A helmet was measured for low velocity impact protection with a helmeted headform drop test. A finite element model of the drop test was developed to incorporate different materials and configurations. Material test data was imported to the drop test model, and the LS-DYNA® model was used to simulate the response of the helmet in the impact test. Based on material test and model simulation results, helmet liner prototypes were fabricated and tested. The effectiveness of crushable foam was demonstrated for a one time use application. A prototype helmet liner combining high density polyethylene (HDPE) foam and viscoelastic comfort foam showed an improvement in impact protection over the current Army Combat Helmet (ACH) system at 4.3 m/s (14 ft/s), although the results were mixed at higher impact velocities.

15. SUBJECT TERMS

FOAM	RIGIDITY	SHOCK TESTS	ENERGY ABSORPTION
BLAST	VELOCITY	IMPACT TESTS	SUSPENSION DEVICES
SHOCK	DROP TESTS	IMPACT SHOCK	IMPACT ATTENUATION
IMPACT	EFFICIENCY	HELMET LINERS	PROTECTIVE EQUIPMENT
LS-DYNA	CUSHIONING	HEAD(ANATOMY)	COMPUTERIZED SIMULATION
HELMETS	PROTOTYPES	TRAUMATIC SHOCK	FINITE ELEMENT ANALYSIS

16. SECURITY CLASSIFICATION OF:			**17. LIMITATION OF ABSTRACT**	**18. NUMBER OF PAGES**	**19a. NAME OF RESPONSIBLE PERSON** John Fitek
a. REPORT	**b. ABSTRACT**	**c. THIS PAGE**			
U	U	U	SAR	56	**19b. TELEPHONE NUMBER** *(include area code)* 508-233-6908

Standard Form 298 (Rev. 8-98)
Prescribed by ANSI Std. Z39.18

This page intentionally left blank

Contents

List of Figures

List of Tables

Acknowledgements

This research effort was funded through the Helmet Electronics and Display System – Upgradeable Protection (HEaDS-UP) Program. The author would like to thank HEaDS-UP Program Manager Mr. Donald Lee for his support. In addition, the author thanks the members of the NSRDEC Ballistics Team for their support and use of the helmet drop test equipment and high speed video camera.

DESIGN OF A HELMET LINER WITH IMPROVED LOW VELOCITY IMPACT PROTECTION

1 Introduction

This report describes a project to design an improved energy absorbing helmet suspension system for low velocity impact protection and to develop the material testing and computational modeling tools required to assist in that effort. This work was performed by the Natick Soldier Research, Development and Engineering Center (NSRDEC), from January to October of 2012. Materials for this project were donated by Team Wendy, Rogers Corporation, and Madison Polymeric Engineering.

The US Army Advanced Combat Helmet (ACH) is a helmet shell for ballistic protection which is suspended and supported on the head by a configuration of foam pads. The ACH can provide low velocity impact protection from a fall or blow to the head if the suspension pads cushion the head and absorb the kinetic energy of the impact. The ACH is currently tested to provide protection at an impact velocity of 10 ft/s, which is equivalent to a vertical drop from approximately 1/2 m. The goal of this project was to use material testing and modeling tools to design and test a helmet liner prototype for increased low velocity impact protection.

Energy absorbing helmet liners are designed by specifying the acceleration limit of the head on impact. The maximum impact protection can be achieved with a material that absorbs energy efficiently by cushioning the head at a level near the acceleration limit. Newton’s laws of motion and conservation of energy can be used with material test data to make an initial assessment of materials for this application.

A finite element model of the helmet and suspension system was developed for this study. LS-DYNA® was used to simulate the impact response of the helmeted headform drop test according to Army and US Department of Transportation (DOT) test specifications. These model simulations were then compared with baseline test results, allowing the model to serve as a tool for designing a helmet liner with improved low velocity impact protection.

2 Background and Theory

2.1 *ACH Suspension System*

The helmet suspension system supports the helmet shell on the head, and can potentially absorb the energy of an impact to the helmet. The ACH suspension system consists of an arrangement of foam pads as shown in Figure 1. The currently fielded suspension system is referred to as the Zorbium Action Pads (ZAP™) and is a product of Team Wendy. The foam material in these pads has the product name Zorbium®, and is viscoelastic polyurethane foam (1). The foam material will absorb energy as it is compressed during an impact to the outer helmet shell.

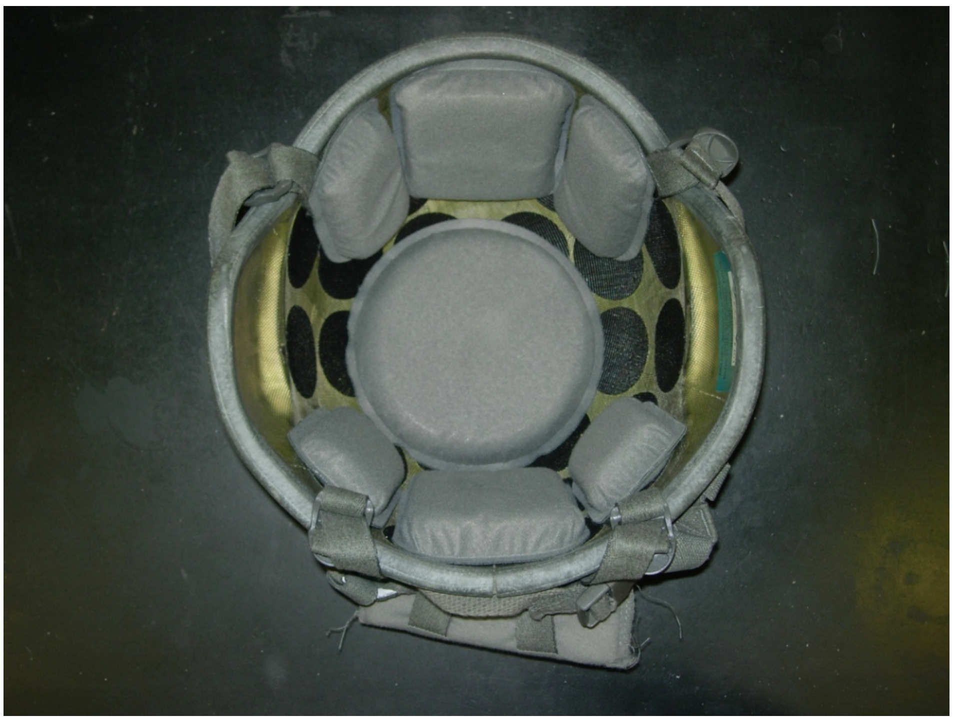

Figure 1: ACH with suspension system pads

2.2 *Energy Absorbing Materials*

Foam is a cellular material that has the ability to deform at a relatively low stress level and absorb energy. Foam is used in protective applications to prevent an object from exceeding a maximum acceleration limit. An example is the use of foam material to package a fragile product for shipment. Foam materials can reduce peak acceleration by reducing the peak force on an object and increasing its duration over time (2). A general stress vs. strain compression curve for a foam material is shown in Figure 2. This diagram shows the three distinct regions of cellular structure response: linear-elastic, plateau, and densification.

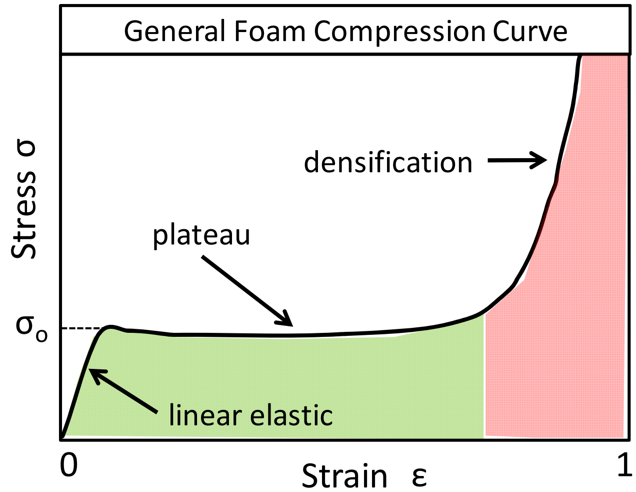

Adapted from (3)

Figure 2. General stress vs. strain response of a foam material

Foam can provide protection from an impact load by absorbing energy through foam compression in the constant stress plateau region, highlighted in green in Figure 2. The foam thickness must be sufficient to absorb the energy of the impact in the plateau region, without compression into the densification region of the foam stress vs. strain curve, highlighted in red (4).

The force acting on the head during impact is equal to the product of the mass and acceleration, as written in Equation 1. The helmeted headform drop test is used to test the ACH for impact protection (5). The test is executed by dropping a head-shaped object, cushioned by the helmet and suspension system, onto a steel anvil. The test specification for the ACH - Large requires limiting the acceleration of the 5 kg DOT-C headform to 150 *g*. Therefore, the force on the headform must be limited to 7350 N.

$$F = ma \qquad \text{(Eq. 1)}$$

The average foam material stress is equal to the force acting on the headform divided by the contact area, as shown in Equation 2. The area will be dependent on the location of impact and the amount of foam compression during impact. For an initial assessment, an impact area of 58.1 cm^2 (3 in x 3 in) will be assumed, which is approximately equal to the front or back pad in the current ACH system.

$$\sigma_{Foam} = \frac{F}{A} \qquad \text{(Eq. 2)}$$

The energy in the impact can be calculated from the initial drop height or the initial velocity of the headform at impact. In Equation 3, *m* is the mass of the headform, *v* is the impact velocity, *g* is the acceleration of gravity, and *h* is the drop height.

$$Energy = \frac{mv^2}{2} = mgh \qquad \text{(Eq. 3)}$$

The kinetic energy absorbed by the foam during impact is equal to the force integrated over the foam compression as seen in Equation 4.

$$Energy\ \ Absorbed = \int F dx \qquad \text{(Eq. 4)}$$

As mentioned previously, the foam must absorb energy in the relatively low stress plateau region. The foam response typically begins to transition from plateau to densification around a compressive strain of 0.65 - 0.70, and the maximum thickness available for the suspension system is assumed to be 19 mm. These parameters are listed in Table 1 and used with Equations 1-4 to predict the required foam stress at different impact velocities. These predictions are listed in Table 2.

Table 1. Simple Model Input Parameters

mass of headform [kg]	5
foam thickness [mm]	19
densification strain	0.65
acceleration limit [g]	150
contact area [cm^2]	58.1

Table 2. Required Foam Stress Predictions

Impact Velocity [ft/s]	Impact Velocity [m/s]	KE [J]	σ_{Foam} [Mpa]
10	3.05	23.2	0.32
14	4.27	45.5	0.63
17	5.18	67.1	0.94
19.8	6.03	90.8	1.27

These simple predictions are used as a basic reference for selecting materials for helmet impact protection. They assume a perfectly plastic material response in the foam under compression. No materials will behave in this ideal manner, and the cushion factor is one way to characterize a material's efficiency as an energy absorber. The cushion factor is the peak stress in the material divided by the energy absorbed per unit volume (3), as written in Equation 5.

$$CF = \frac{\sigma_P}{W} \qquad W = \int \sigma \, d\varepsilon \qquad \text{(Eq. 5)}$$

A perfectly plastic energy absorber would have a cushion factor of 1.0, and materials can be compared for energy absorbing efficiency based on the cushion factor. The cushion factor can be plotted against the peak stress in the foam material as shown in Figure 3.

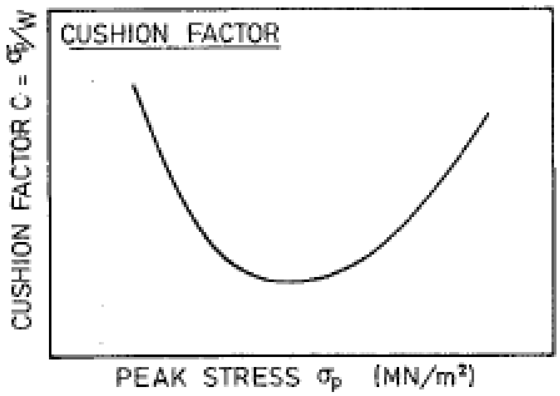

Figure 3. Cushion factor plotted vs. peak stress (3)

Materials that are not perfectly plastic will return some of the energy they absorb during a rebound phase. The difference between the loading and unloading curves during impact is a measure of the energy dissipated, or hysteresis, as shown in Figure 4.

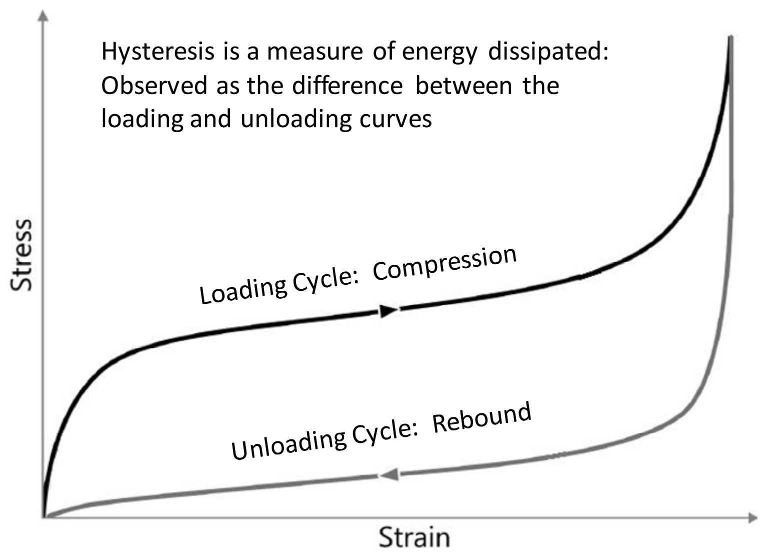

Adapted from (6)

Figure 4. Loading and unloading curves: hysteresis

The hysteretic unloading ratio is the amount of the rebound energy divided by the total energy absorbed. A material which instantly rebounds from its compressed state will increase the total duration of the impulse on the headform and will increase the total change in momentum of the headform. Although the usage of a peak acceleration limit as a pass/fail criteria does not account for this, a material which causes the headform to rebound could have a negative effect on protection.

3 Methods

In this study, a variety of foam materials were tested and assessed for application in a helmet suspension system/energy absorbing liner (Table 3).

Table 3: Materials for Testing

Manufacturer	Foam	Type/ID	Polymer Material	Flexible/Rigid	Energy Abs. Mechanism	Density		Quasi-Static Comp. Strength
						kg/m^3	lb/ft^3	Mpa
Evonik	Rohacell	31A	Polymethacrylimide	rigid	brittle fracture	32	2.0	0.40
Evonik	Rohacell	51A	Polymethacrylimide	rigid	brittle fracture	52	3.2	0.90
Zotefoam	Plastazote	HD60	HD Polyethylene	semi-rigid	elastic/plastic	60	3.7	0.35
Zotefoam	Plastazote	HD80	HD Polyethylene	rigid	elastic/plastic	80	5.0	0.50
Zotefoam	Plastazote	LD45	LD Polyethylene	flexible	elastic/plastic	45	2.8	0.12
Zotefoam	Plastazote	LD70	LD Polyethylene	flexible	elastic/plastic	70	4.4	0.20
Team Wendy	Zorbium	Z110i	Polyurethane	flexible	viscoelastic	54	3.4	0.07
	EPS	2lb	Polystyrene	rigid	elastic/plastic	32	2.0	0.25

ROHACELL® is a rigid, lightweight foam with a closed-cell structure and a very high strength-to-weight ratio (7). It is primarily used as a sandwich composite core in the aerospace industry. PLASTAZOTE® materials are closed cell polyethylene foams, commonly used for protective equipment for sports, including application in helmet liners (8). Zorbium® is the viscoelastic polyurethane foam in the currently fielded ACH suspension system pads (1). Unlike these more specialized materials, expanded polystyrene (EPS) is a common packaging material that is tested for comparison.

The materials were chosen for testing based on a literature search, manufacturer's data sheets, or current usage in similar applications. These materials were impact tested so the material test data would be obtained at applicable impact rates. The data were used to screen the materials for further testing and analysis.

A finite element model of the helmeted headform drop test was developed for this study using LS-DYNA®. Materials that show the desirable combination of compressive strength and energy absorbing efficiency were modeled with LS-DYNA® and imported into the helmeted headform drop test model. The model was then used to predict the performance of the material as a helmet suspension pad or helmet liner material.

ACH shells were fitted with the foam materials that showed the highest predicted performance from the material test and model simulations. The prototype testing was used to determine if the new system was an improvement on the currently fielded system. A flowchart of the research methodology is shown in Figure 5.

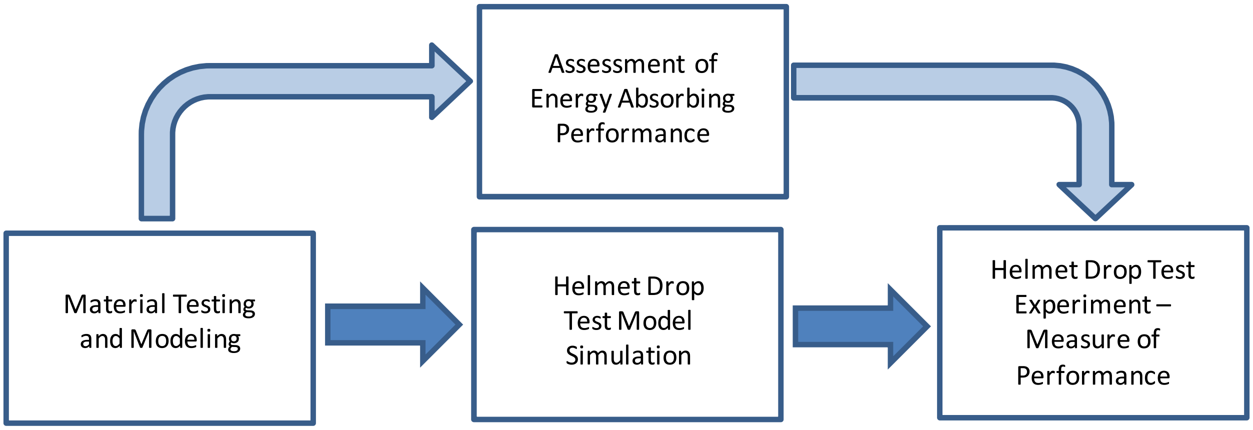

Figure 5. Flow chart of model and test plan

3.1 *Material Testing*

An instrumented drop weight impact test is a relatively simple experiment which can measure the stress vs. strain response and energy absorption properties of foam materials. In this project, the monorail drop test device, used for the helmeted headform drop test, was modified for material testing as shown in Figure 6. . The headform was replaced with a flat faced steel striker, and the hemispherical anvil was replaced with a steel anvil and dynamic load cell assembly.

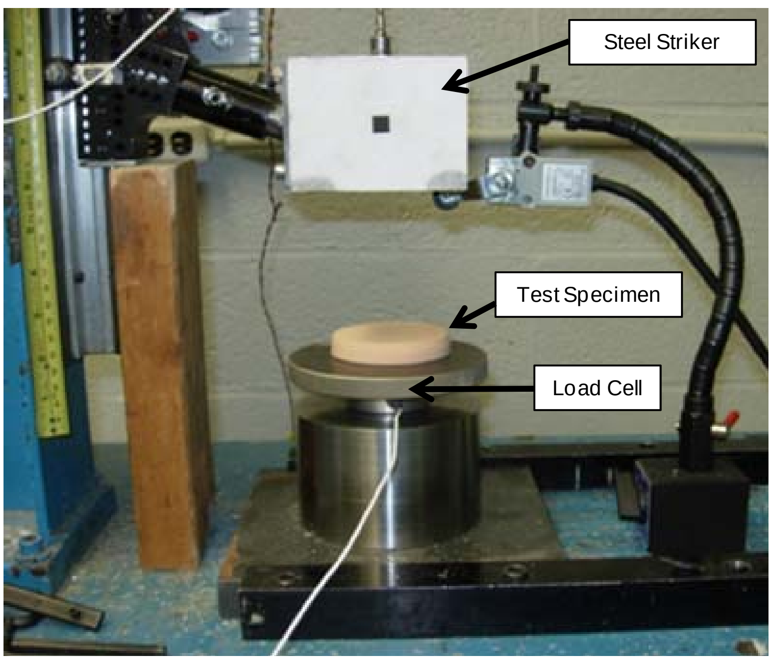

Figure 6. Drop weight impact test set-up

The drop weight impact test for materials includes a steel striker, which compresses the foam material between a steel anvil during impact. The striker is instrumented with an accelerometer, and the anvil is instrumented with a dynamic load cell. A high speed camera is used to capture video of the impact test. A contact switch is used to simultaneously trigger both the data acquisition system and the video camera. The test specifications and data acquisition equipment specifications of the drop weight impact test are listed in Table 4.

Table 4. Impact Test Data Acquisition and Sensor Information

Steel Striker Dimensions Striker Mass	102mm x 102 mm x 76mm (4"x4"x3") 7.3 kg
Specimen Diameter Specimen Area	76.2 mm 45.6 cm^2
Data Acquisition Sys. Data Sampling Rate	Nat. Inst. USB-6251 / Matlab 10 kHz
High Speed Video Camera Frame Size Frame Rate	Vision Research Phantom V710 512 X 512 10k frames/sec.
Dynamic Load Cell Load Cell Capacity Signal Conditioner	PCB 200C20 0 - 88.96 kN (20,000 lbs) PCB Model 482A22
Accelerometer Accelerometer Range Signal Conditioner	Kistler 8704B500 +/- 500 g Kistler Type 5114
Triggering	Hardware Trigger - signal from contact switch simultaneously triggers DAQ and Camera

A stress vs. strain compression curve is created from the instrumented drop weight impact test with high speed video. Stress in the foam is equal to the force measured by the load cell, divided by the specimen surface area. The compression of the foam is measured by tracking the black square (located at the center of the striker) in the high speed video after it makes contact with the foam surface, as shown in Figure 7. This is accomplished through use of the MATLAB® Image Analysis Toolbox™.

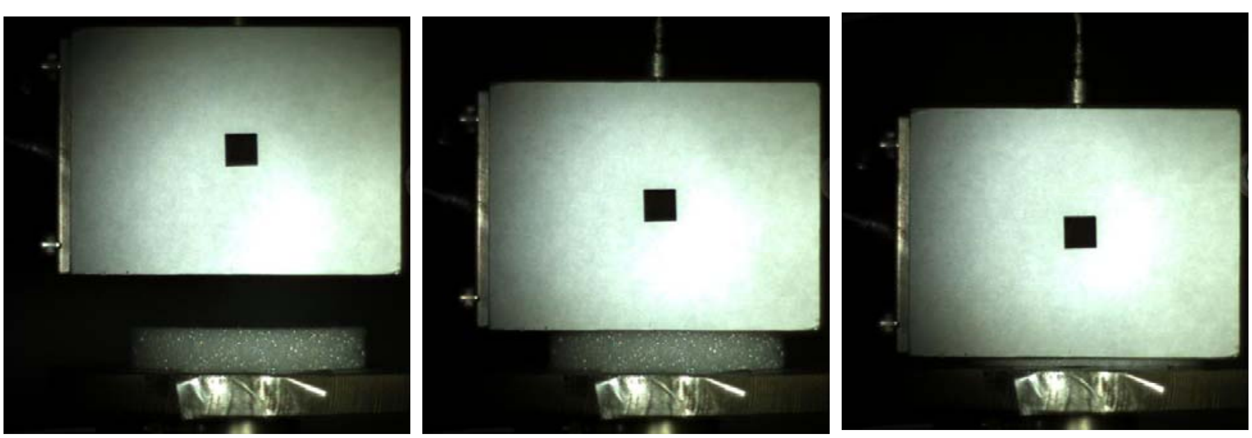

Figure 7. Drop weight impact video frames

Because the high speed video camera and the data acquisition system are triggered by a contact switch which is triggered before impact, the video is synchronized with the sensor measurements. The first frame must be determined by observing the video frames and data points just at the point when the striker makes contact with the foam test specimen surface. Based on these analysis steps, a stress vs. strain curve for the foam material in the impact test is generated.

3.2 ***Computational Modeling***

3.2.1 Finite Element Mesh Generation

The helmet mesh (29376 elements) was created from a scan of an ACH-Size Large (9) using TrueGrid®, a finite element mesh generation and pre-processing software package. Helmet pad footprints are defined using geometric planes and shapes using TrueGrid®. The pad thickness is created by extruding the footprints towards the center of the helmet with the LS-PrePost®. The pads can be projected onto the inside surface of the helmet scan, or simply placed into position and pressed into the helmet by the headform during an initialization step of the model simulation. The helmet mesh and projection of foam pad geometry is shown in Figure 8.

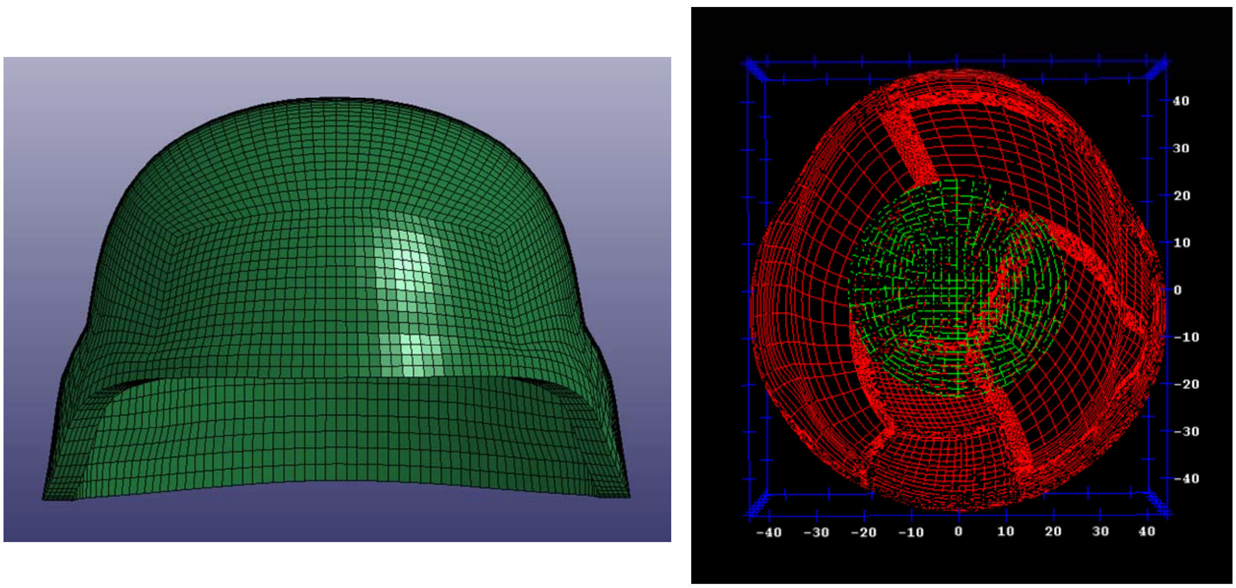

Figure 8. Helmet and foam pad mesh generated with TrueGrid® and LS-PrePost®

This geometry and mesh generation technique allows for the foam pads to be resized and repositioned within the helmet by specifying new geometry and rapidly re-meshing the parts. It also allows for the design and modeling of new helmet suspension system configurations. The standard pad configuration (10) and an alternative experimental design are shown in Figure 9.

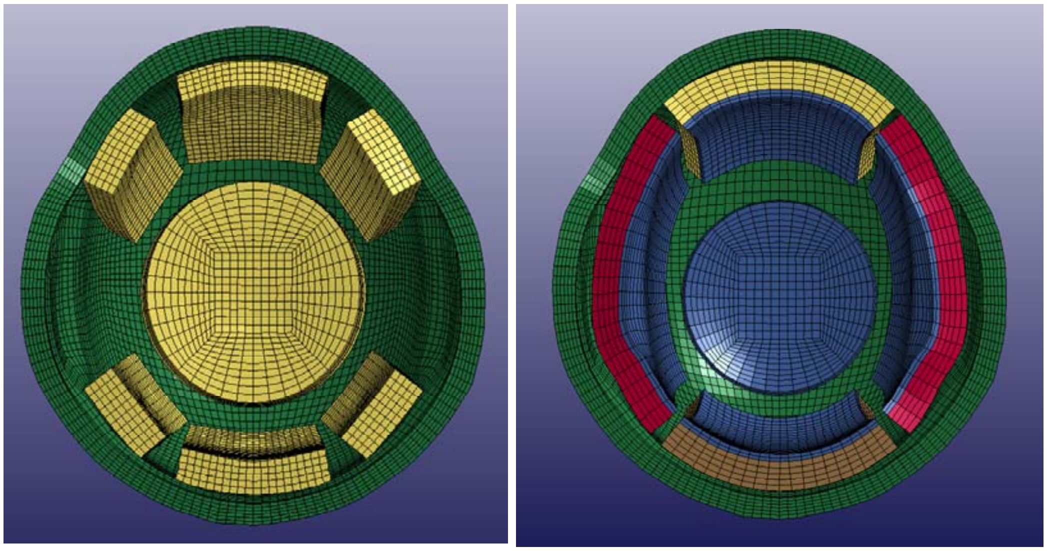

Figure 9. Suspension system models designed and meshed with True Grid® and LS-PrePost®

The headform mesh (73728 elements), displayed in Figure 10, was created from a scan of the DOT-Size C headform (9). The large number of elements were used in the headform model to improve the contact between the headform and foam pads. Despite the refined mesh, the headform model has a low computation time cost because it is modeled as a rigid body.

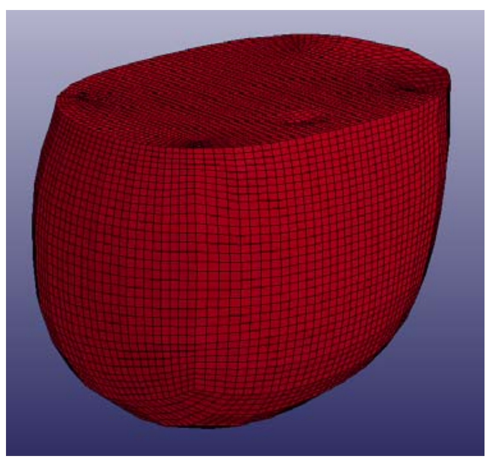

Figure 10. Mesh of DOT-C headform

3.2.2 Helmeted Headform Impact Model

The magnesium headform and steel anvil are modeled as rigid materials in LS-DYNA®. Stress and strain in the parts are not calculated, as LS-DYNA® does not allow deformation in a rigid part. The density and Young's modulus are included in the rigid material model for momentum and contact analysis.

The headform mesh does not include the full detail of the DOT headform or the additional mounting hardware. The density of the headform in the model is adjusted slightly (from 1.77 kg/m^3 to 1.64 kg/m^3) to result in a total mass of 5 kg, to match the DOT-C headform assembly in the drop test experiment.

The composite helmet is modeled with an isotropic elastic-plastic material model (11). An orthotropic composite material model with damage was also considered (12), but due to its increased complexity and the inability to validate the model, the simpler isotropic model was more appropriate for this study. The impact response of the composite helmet shell may have a significant effect on the low velocity impact response of the complete helmet system. Further study in this area is recommended to improve the accuracy of the model predictions.

LS-DYNA® is used to simulate the impact of the helmeted headform onto a hemispherical steel anvil. There are five different headform orientations in the ACH impact test. Four of these impact positions were modeled in this study, as displayed in Figure 11.

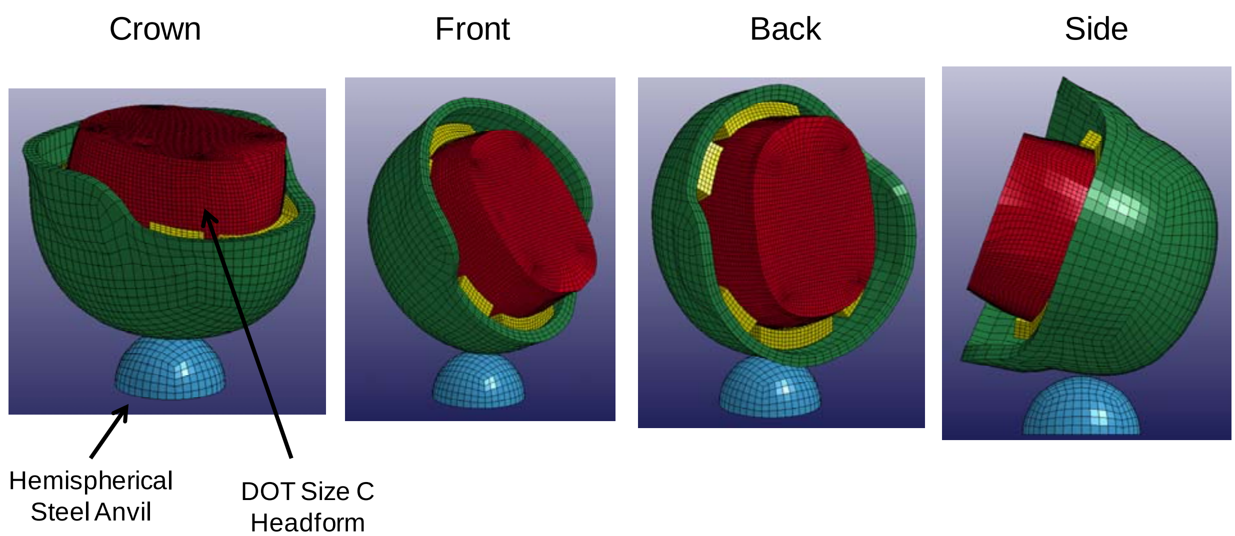

Figure 11. Helmet and headform positioning for impact simulations

Before the impact simulation can be executed, an initial step must be conducted to position the headform in the helmet and pre-compress the foam pads. To model the current ACH pad configuration, the non-deformed foam pads are placed into position in the helmet and pressed against the inside of the helmet by the headform. The initial and final positions of the headform and initial compression of the foam pads are shown in Figure 12.

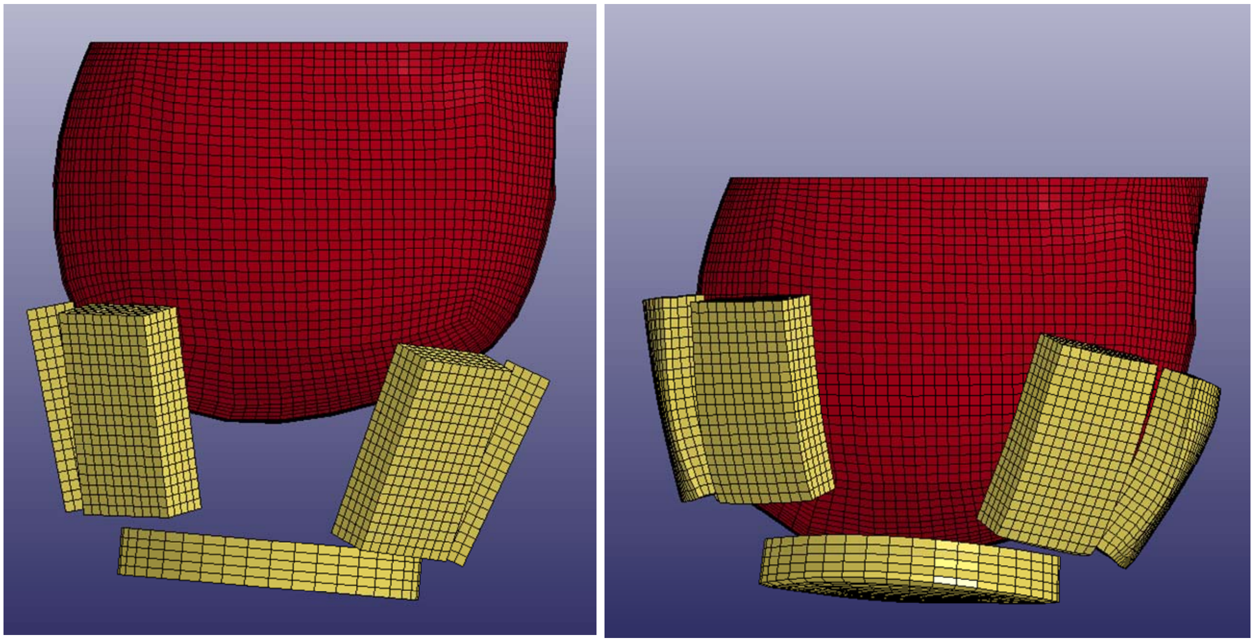

Figure 12. Fitting the headform into the helmet and pads

When the headform is in position, the initial simulation step is terminated. The simulation is then restarted with the headform in position with an initial compression on the foam pads. At the initiation of the restart, the initial velocity of impact is applied to the helmet, foam pads, and headform. The helmet is located within mm of the hemispherical anvil, so the impact occurs within 1 ms after the restart.

A discrete spring element is added during the restart simulation in the front, back, and side impact simulations as shown in Figure 13. This part was put in place as a simple retention system to prevent the helmet from coming off the headform during the simulation, while still allowing helmet displacement and rotation with respect to the headform.

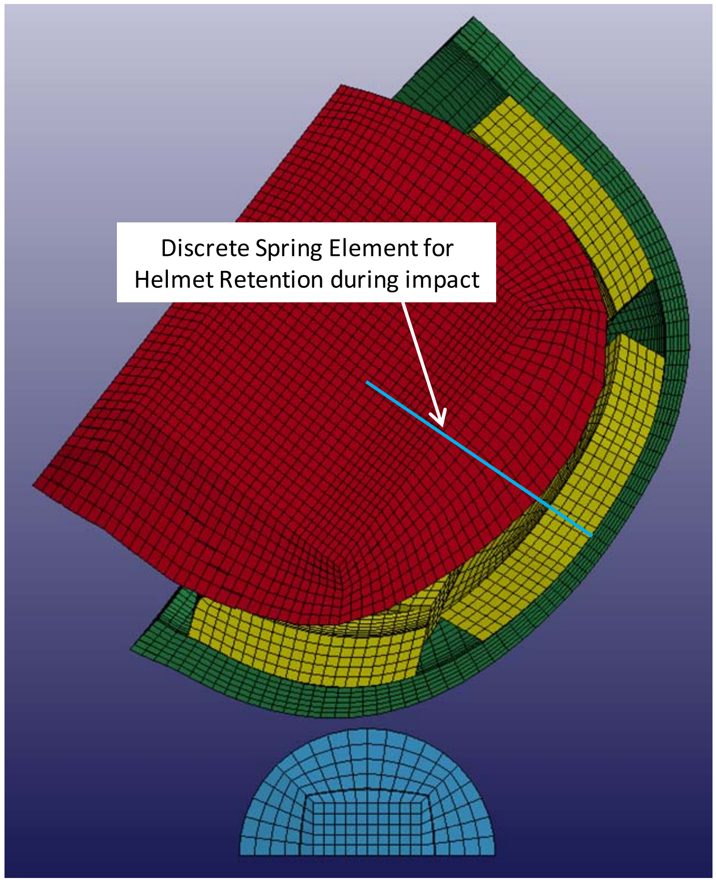

Figure 13. Discrete spring element for helmet retention

A partial list of the LS-DYNA® keywords, a list of material model parameters, and experimental stress vs. strain curves for input to the foam models are provided in Appendix A.

3.3 ***Helmet Testing***

3.3.1 Experimental Set-up

Helmets were tested for low velocity impact protection in a guided free fall drop test using a monorail drop test apparatus as shown in Figure 14. All helmets tested in this study were ACH-Size Large and were tested on the appropriate DOT-Size C headform. The headform is constructed of K1A Magnesium alloy and instrumented with a Kistler accelerometer model 8704B500 with a linear measurement range of +/- 500 *g*. All tests were conducted on a hemispherical steel anvil (4.8 cm radius). A laser and an optical sensor were used to measure the impact velocity with a gate that passed between them. The data acquisition system was the same as described for the drop weight impact test for materials, but included a data filter applied through the MATLAB® Signal Processing Toolbox™ (4-pole Butterworth low pass filter with a 1 kHz cut-off frequency).

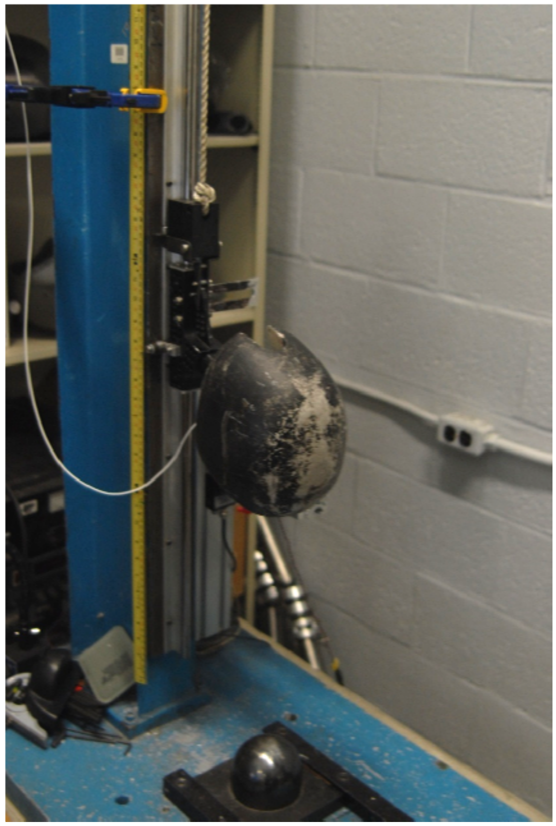

Figure 14. Monorail drop test with DOT-Size C headform and hemispherical anvil

When combined with an environmental conditioning chamber, this set-up is capable of testing helmets for blunt impact protection as described in the ACH CO/PD-05-04 (Paragraph 4.10.13) (5), which references the DOT Test Specification 571.218 (13). In this study, helmets were tested at ambient conditions and at the hot condition. For the hot condition, helmets were conditioned overnight at 54 °C (130 °F). They were removed from the conditioning chamber and tested in the ambient environment within 5 min. The helmet was returned to the conditioning chamber for 15 min before subsequent tests.

3.3.2 Helmet Suspension System Prototyping

Several different techniques were used to build prototype helmet suspension systems designed for low velocity impact attenuation. One technique was to remove the foam material from an existing suspension system pad and replace it with a different foam material. This technique has the advantage that the foam material being tested can be compared with existing pad systems by maintaining the same pad size and position. The standard pad configuration (10) is displayed on the left side of Figure 15, and an experimental prototype is on the right.

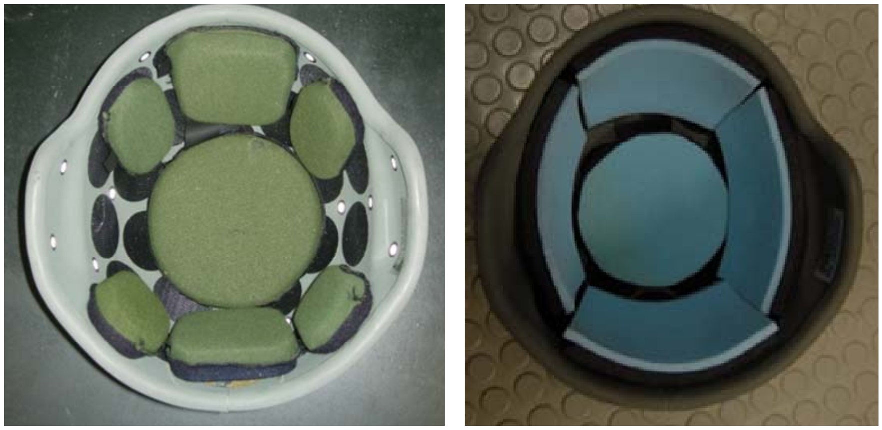

Figure 15. ACH pad configuration. Left: Standard configuration Right: Experimental prototype

It may be desirable to have the suspension system provide increased areal coverage in the space between the helmet and the head. Increased coverage could engage more energy absorbing material during impact. Within the scope of this project, it was impossible to create a full helmet liner with most foam materials because a full helmet liner requires a mold and most foam materials are usually only available in sheet form. As an alternative, the foam materials were cut and arranged in the helmet to create a partial helmet liner. This was done by cutting pieces of foam (water jet cut or die cut), forming them to the shape of the inside of the helmet and fixing them with adhesive as shown on the right side of Figure 15.

4 Results and Discussion

4.1 *Material Test Results and Analysis*

The results of the material tests are shown in Table 5. The stress vs. strain response from the material test was used to calculate the dynamic compression strength, hysteretic unloading ratio, and the minimum cushion factor. In addition, the stress vs. strain response was used to calculate the predicted energy absorbed according to the theoretical model described in Section 2.2. Table 5 displays the amount of energy absorbed up to the 150 *g* acceleration limit. The column to the right indicates the maximum impact velocity that could be reached with this material, based on that assessment. This initial analysis indicated that the ROHACELL® 51A could be used with impact velocities nearing 5.2 m/s (17 ft/s), and the PLASTAZOTE® HD80 had the energy absorbing capacity for impact velocities of approximately 4.3 m/s (14 ft/s).

Table 5. Material Impact Test Results

Type/ID	Density	Quasi-Static Comp. Strength	Approx. Impact Strain Rate	Dynamic Comp. Strength	HU ratio	CF min	Energy @ 150g Accel Limit	Max Impact Velocity	
	[kg/m³]	[Mpa]	[1/s]	[Mpa]			[J]	[m/s]	[ft/s]
Ro-31A	32	0.40	2.0E+02	0.40	0.08	1.3	37.2	3.9	12.6
Ro-51A	52	0.90	3.1E+02	0.95	0.03	1.2	80.2	5.7	18.6
HD60	60	0.35	2.0E+02	0.37	0.31	2.3	42.0	4.1	13.5
HD80	80	0.50	2.7E+02	0.60	0.18	2.0	55.7	4.7	15.5
LD45	45	0.12	1.9E+02	0.11	0.87	2.7	22.7	3.0	9.9
LD70	70	0.20	2.1E+02	0.23	0.51	2.7	32.8	3.6	11.9
Z110i	54	0.07	2.0E+02	0.25	0.23	2.2	31.9	3.6	11.7
EPS-2.0	32	0.25	1.9E+02	0.25	0.35	2.5	33.9	3.7	12.1

Different drop heights are required to reach full compression of the materials, resulting in different testing rates. Therefore, strain rate for each test is listed with the results. The dynamic strain rates were very similar to the manufacturers' reported quasistatic rates, with the exception of the Z110i polyurethane foam.

Viscoelastic polyurethane foam material has a glass transition temperature near ambient temperature. The polymer structure will stiffen at higher rates of deformation. This can provide excellent impact attenuation results at ambient temperature, but will result in a softer material at higher temperatures. Although the temperature and rate sensitivity are most drastic with viscoelastic foam, all materials for this application should be studied for temperature and rate effects. Such study was outside the scope of this project. However, some of the helmet prototypes in this study were conditioned at 54 °C (130 °F) to account for loss of strength at elevated temperatures, according to the ACH Purchase Description.(5).

In addition to the dynamic compression strength, the results include the hysteretic unloading ratio and the minimum cushion factor, as described in Section 2.2. The results show that the ROHACELL® foams are the most efficient energy absorbers, and the brittle cell fracture mechanism returns very little energy with nearly zero rebound. The downside of this material is that it can be used for only one impact if it reaches its energy absorbing capacity.

Despite this negative aspect, it was valuable to demonstrate the effectiveness of this material (14), while considering other options. The stress vs. strain impact responses of ROHACELL® 31A (32 kg/m^3) and 51A (52 kg/m^3) are shown in Figure 16. The listed compressive strength levels of these materials are 0.4 MPa and 0.9 MPa, respectively, which are very similar to the dynamic strength measured in the impact test. This shows the material has a low degree of rate dependence within this range.

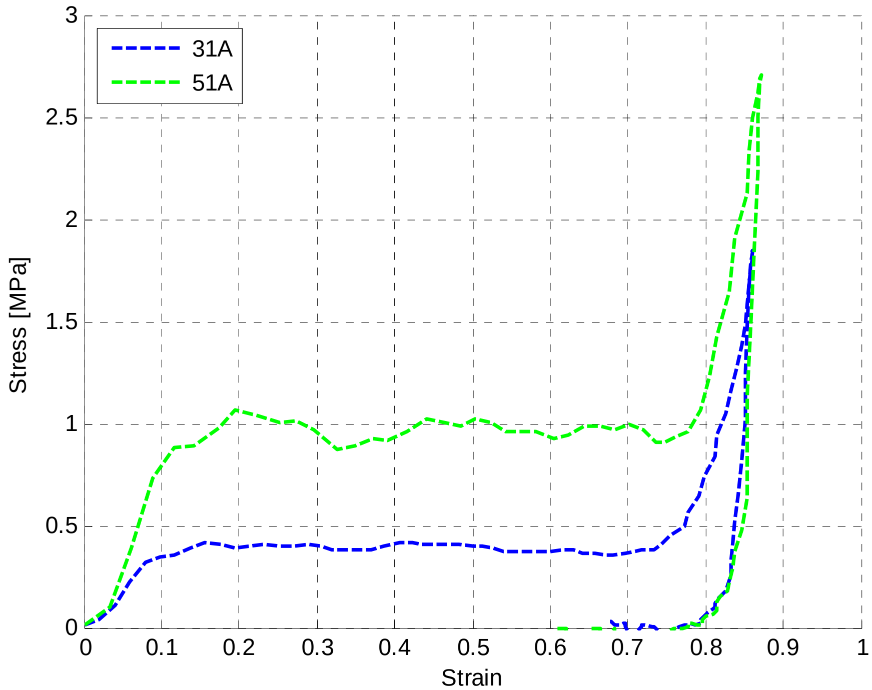

Figure 16. ROHACELL® foam stress vs. strain compression curves

The PLASTAZOTE® high density polyethylene (HDPE) materials showed a favorable combination of properties. They had relatively high compression strength levels, theoretically have more temperature stability than viscoelastic foam, and although not fully recoverable remained intact after impact. Figure 17 shows the stress vs. strain response of the two HDPE foam densities in the impact test.

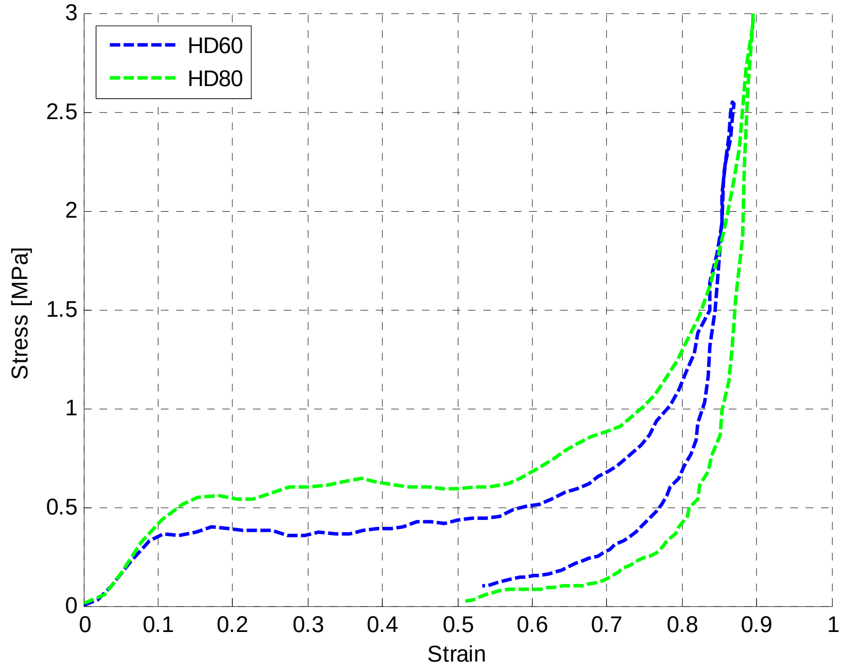

Figure 17. PLASTAZOTE® HDPE stress vs. strain compression curves

Although these materials do not show the ideal plateau stress shown by the ROHACELL® materials, they are relatively efficient energy absorbers. Figure 18 shows a comparison of the PLASTAZOTE® HD60 to the ROHACELL® 31A, which have very similar plateau stress levels.

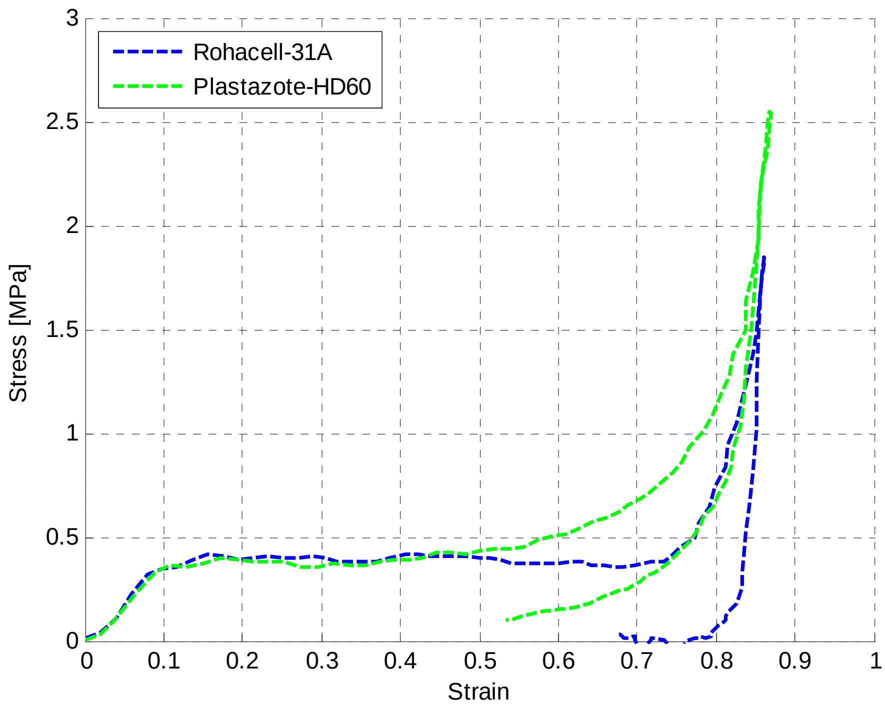

Figure 18. Comparison of foam materials with similar compressive strength

Based on the material test results, modeling and prototyping of a helmet liner for improved low velocity impact protection was pursued with the ROHACELL® and PLASTAZOTE® HDPE materials.

4.2 *Computational Modeling*

4.2.1 Model of the Current ACH System

The first step after creating the model of the helmet and suspension system was to simulate the response of the current system and compare the results with baseline test data. An ACH suspension system pad was tested in the drop test to capture the stress vs. strain results. These results were imported to an LS-DYNA® foam material model (6): *MAT_LOW_DENSITY_FOAM. A simulation of the material drop test was used, and the hysteretic unloading was entered into the material model. A model parameter which controls the shape of the unloading curve was fit to match the unloading behavior in the experiment. The drop test simulation with the curve fit model and the material test response are plotted together in Figure 19.

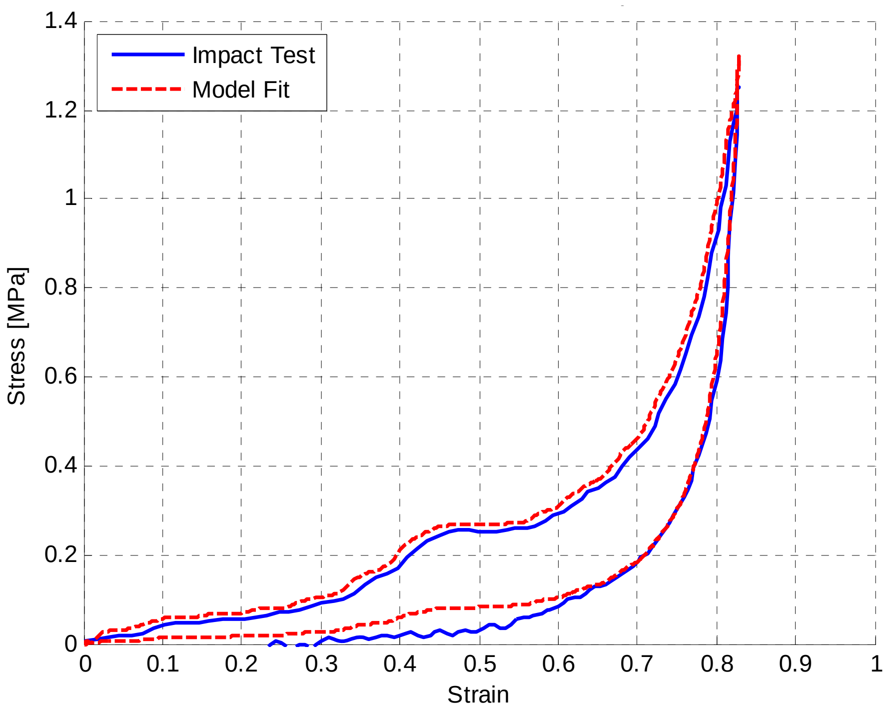

Figure 19. Compression of ACH pad with LS-DYNA® model curve fit

The material model is imported to the model of the helmet drop test with the standard pad configuration. The model simulation results are compared to the baseline data provided by Technical Management Division (TMD),Project Manager Soldier Protection and Individual Equipment (PM-SPIE) (15) (16) as displayed in Figure 20 and Figure 21. The baseline data displayed are an average of a minimum of six tests at an ambient temperature of 22 °C.

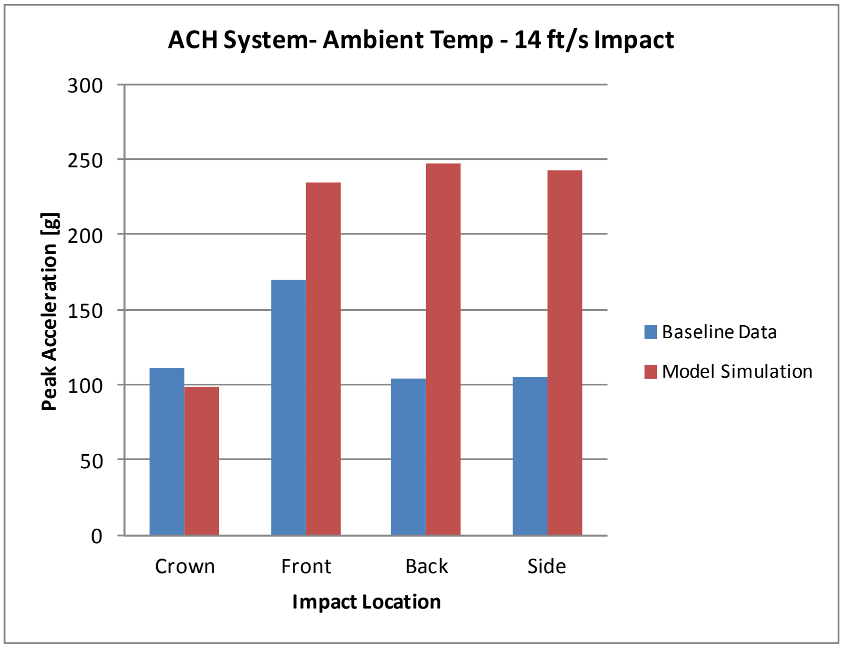

Figure 20. Comparison of simulation and experiment for current ACH system at 4.3 m/s (14 ft/s)

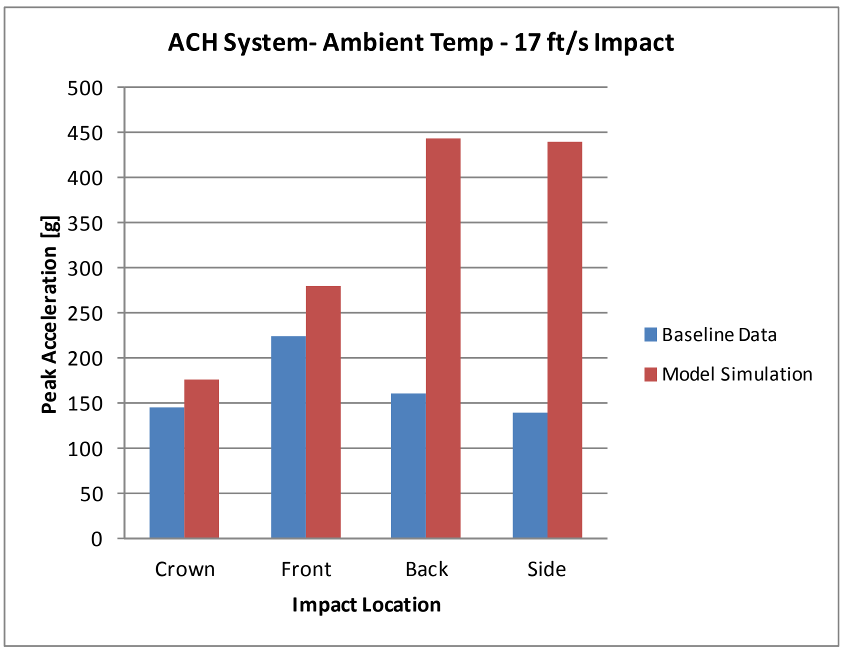

Figure 21. Comparison of simulation and experiment for current ACH system at 5.2 m/s (17 ft/s)

The correlation between the model and experiment varied significantly depending on the impact location and impact velocity. Figure 22 shows the superposition of the experimental acceleration and the simulated acceleration for the crown impact position at 5.2 m/s. In this case, the model and experiment correlated well.

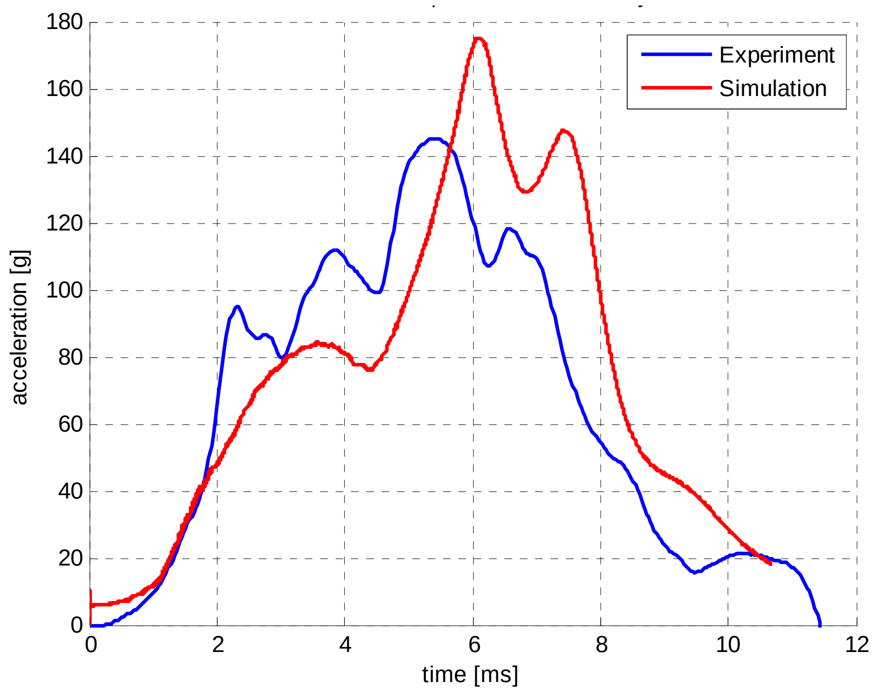

Figure 22. Comparison between model and experiment of crown impact at 5.2 m/s (17 ft/s)

Some of the oscillations observed in the simulated acceleration trace were the result of the helmet bouncing off the anvil during impact. This bouncing was most noticeable in the crown location impact test, and highlights the importance of the helmet response in the resulting headform acceleration.

In the back location impact, there was not as close a correlation between the model and the experiment. The simulation and experimental data deviate as they approach peak acceleration, as shown in Figure 23. The model showed a rapid increase in acceleration as the foam pad was compressed into the densification region.

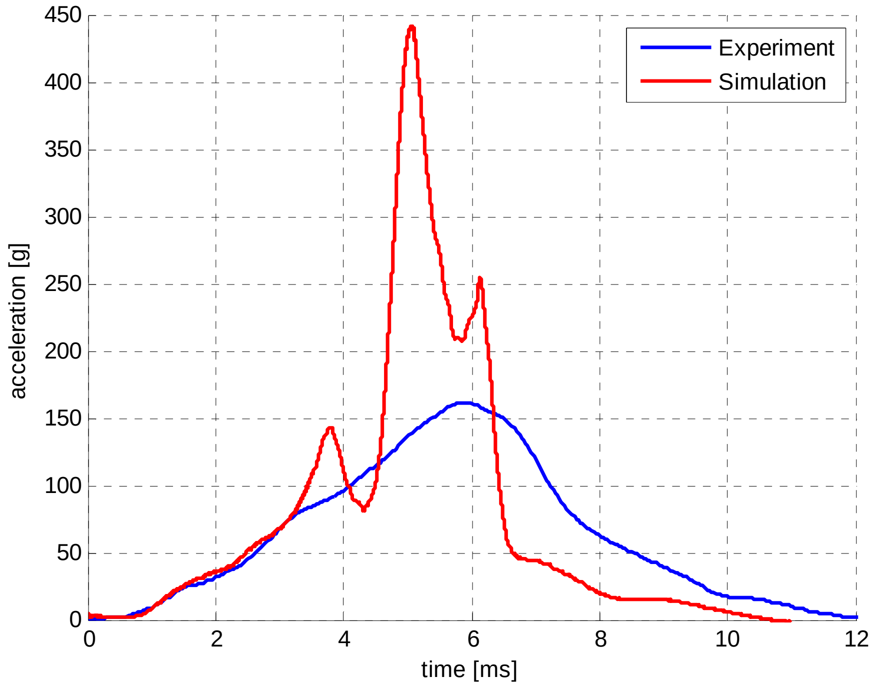

Figure 23. Comparison between model and experiment of crown impact at 5.2 m/s (17 ft/s)

There were several factors which contributed to the deviation between the simulated and experimental helmet impact responses. One reason for this difference in response between the model and experiment could be due to temperature effects of the foam pad. The material response of the pad was measured in at an ambient temperature of 25 °C, while the baseline helmet data test was conducted at an ambient temperature of 22 °C.

Another reason for the higher accelerations in the model simulation could be the simple spring retention system used in the model. Particularly in the front and side location impacts, the helmet tends to rotate on the headform after the initial impact, which significantly changes the positioning of the foam pads with respect to the headform. This change of position can reduce the area of the foam pad which is engaged between the helmet and headform. An improved model of the helmet retention system would improve the accuracy of the simulations.

Deviation between the model and experiment could also be due to differences in the response of the helmet material. In the experiment, the helmet deforms and undergoes permanent damage on impact, especially at the 5.2 m/s impact velocity. The helmet shell response can have a significant effect on the overall helmet and suspension system impact performance. An isotropic elastic-plastic material model is used to model the composite helmet shell (11). The accuracy of the model predictions could be improved through a validated composite material model, with orthotropic strength and stiffness properties. Despite the inability to accurately predict the peak acceleration for all impact locations, the model will be used as a design tool and reference for prototyping and testing efforts.

4.2.2 Model Used to Find Desired Material Strength

The model was used to identify the optimum foam strength for the back location impact at 5.2 m/s. The back location impact was used for this analysis because model simulation results showed the highest peak acceleration with this position. A general foam model was used to represent the foam material in LS-DYNA®, where the foam strength can be scaled to the desired value. The foam pads are positioned in the ACH standard configuration. The thickness of the pads is equal to 22 mm, equivalent to the total thickness of the ACH pads. The results of the parametric study are shown in Figure 24.

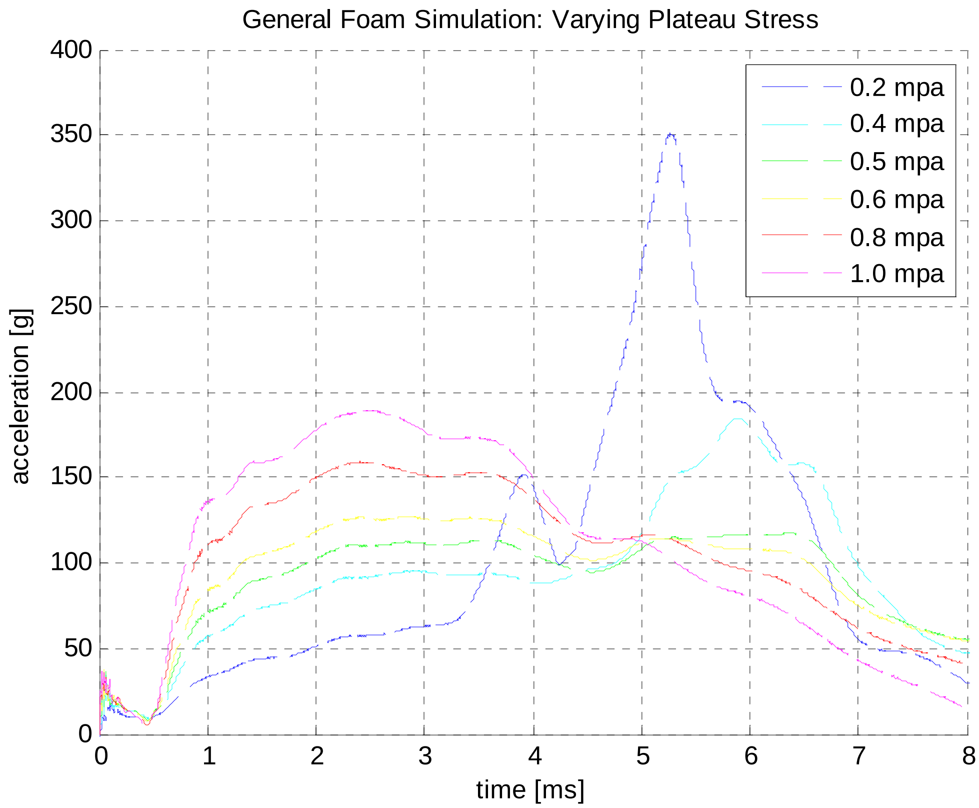

Figure 24. Simulation of back location impact and varying foam strength

The results show that the 0.8 MPa strength foam would be the optimum material strength because it causes a relatively constant headform acceleration of 150 *g*. The lowest strength model of 0.2 MPa "bottomed out" by reaching densification, resulting in a sharp acceleration peak. The material models of 0.5 MPa and 0.6 MPa did not bottom out with a sharp acceleration peak, but they did not absorb energy near the 150 *g* acceleration limit.

4.3 *Helmet Testing*

The overall NSRDEC test results are compared to baseline test data for the current ACH helmet system in Figure 25 and Figure 26 at 4.3 m/s (14 ft/s) and 5.2 m/s (17 ft/s) impacts, respectively. The baseline data were provided by TMD-PM-SPIE (15) (16). The baseline data are the average of a minimum of six tests for each configuration (impact location and velocity) on previously untested helmets. The NSRDEC data are an average of two tests on helmets which have been previously tested, some of which showed visible damage at the impact site. Impact data at the crown, front, and back locations were used for comparison.

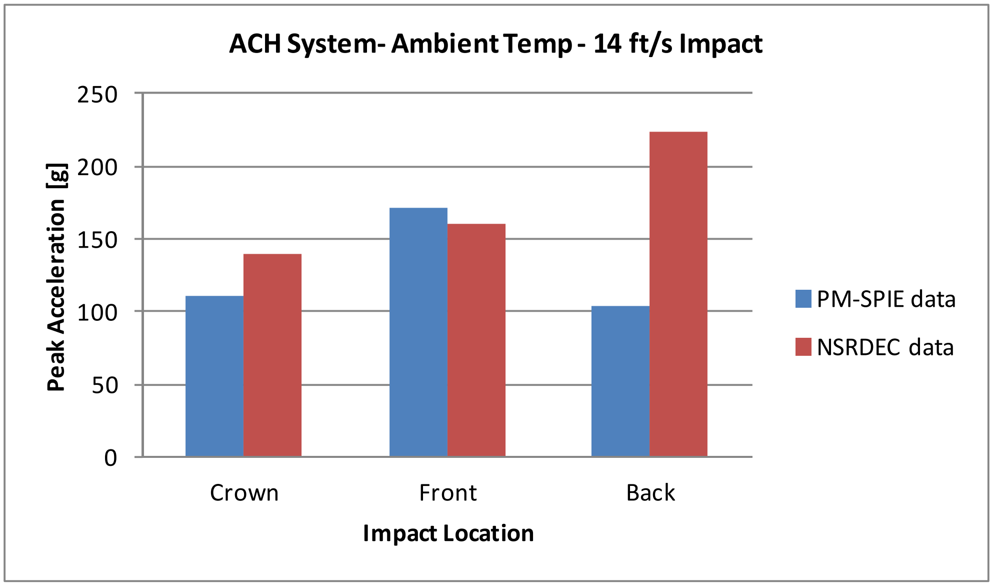

Figure 25. Comparison of data from PM-SPIE and NSRDEC at 4.3 m/s (14 ft/s)

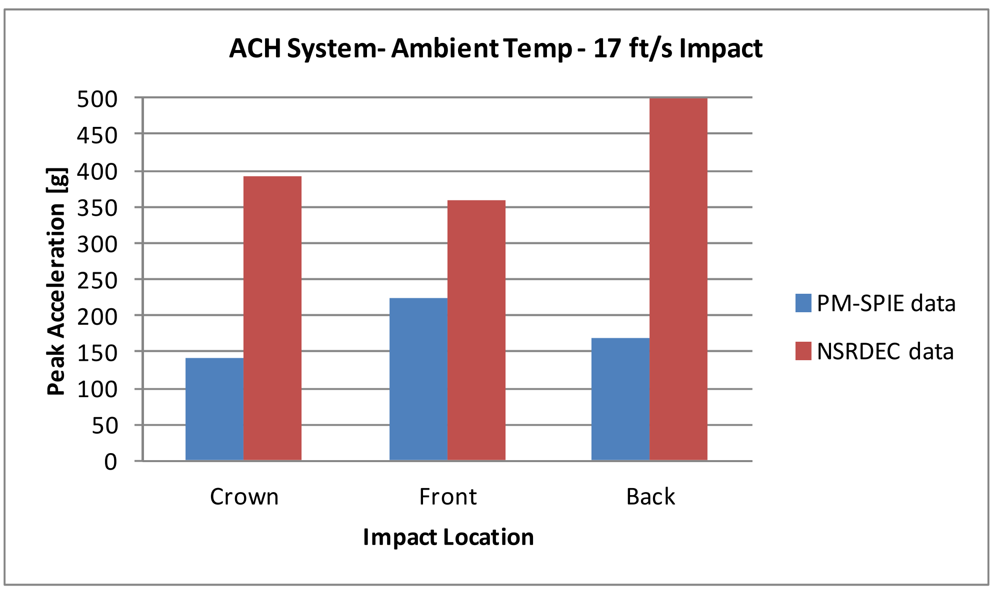

Figure 26. Comparison of data from PM-SPIE and NSRDEC at 5.2 m/s (17 ft/s)

For all but the front location impact at 4.3 m/s, the NSRDEC results show higher accelerations than the baseline. The NSRDEC results are exceptionally higher for all impact locations at 5.2 m/s The baseline data shows the front location impact having higher accelerations than the back location impact, while the opposite is true in the NSRDEC data.

As in the comparison between the model and baseline data, some of these differences may be attributed to different ambient temperatures. The NSRDEC testing of the ACH system was conducted at an ambient temperature of 26 °C, while the baseline data were collected at 22 °C. Another significant difference is that the NSRDEC experiment required re-using helmet shells which were previously tested. In some cases, these helmet shells already showed some visible damage before testing. It is important to highlight these differences in the experiments. Despite these irregularities, the NSRDEC testing were used in this study to make a preliminary assessment of helmet prototype performance, and to make comparisons with model predictions.

4.3.1 Crushable Foam Pad-Replacement Prototype

The material testing and modeling work shows that the ROHACELL® 51A could potentially provide protection at impact velocities of up to 5.2 m/s at the front and back impact locations. When the contact area is larger, such as in the crown impact position, lower strength foam could be required. In this study, both ROHACELL® densities were tested in helmet prototypes using the standard pad configuration. The foam thickness was 19 mm, and a fresh set of pads was used for each impact test. The ROHACELL® foam is placed into the fabric covering of an ACH pad as shown in Figure 27.

Figure 27. ROHACELL® foam replaced in fabric pad covering

The test results at 5.2 m/s impact for two ROHACELL® foams in four locations of the helmet prototype are displayed in Table 6. Graphs of the acceleration traces for the front, back, crown, and side impacts at 5.2 m/s are provided in Appendix B, including comparison with model simulations.

Table 6. Preliminary Tests Using Two Different ROHACELL® Foams at 5.2 m/s Impact

Impact Location	Peak Acceleration (*g*/s)	
	ROHACELL 31A	ROHACELL 51A
Rear	344	144
Front	141	121
Crown	129	204
Side	300	112

The compressive strength of the 31A material is too low for the back and side impact locations, although it did limit the acceleration to 150 *g* in the front and crown impact locations. For all impact locations except for the crown, 51A had less acceleration than 31A. A comparison of the acceleration traces at the back impact location with both foam densities is shown in Figure 28. The 51A foam limited acceleration to 150 *g* while the 31A foam showed a sharp spike in acceleration nearing 350 *g*.

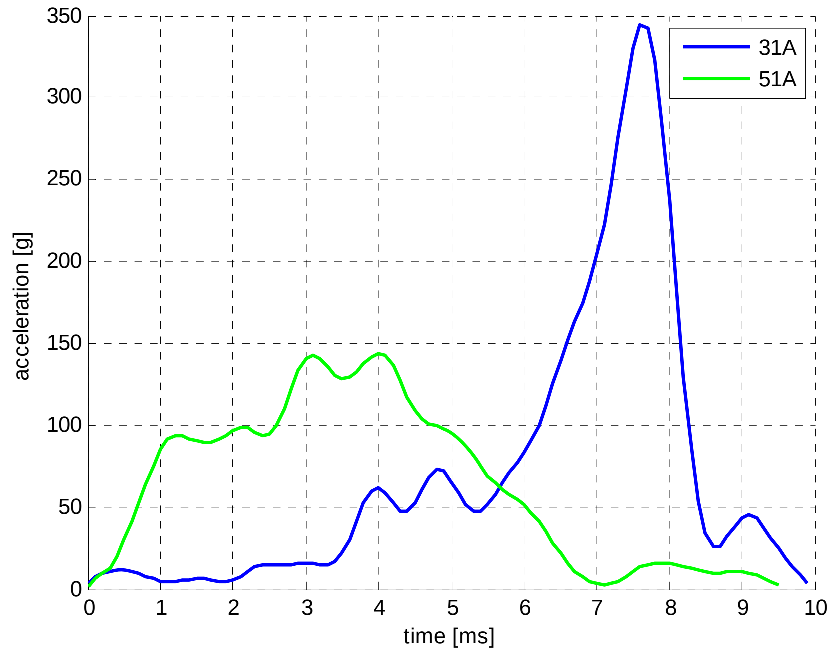

Figure 28. Back location impact with ROHACELL® foam, 5.2 m/s (17 ft/s)

The opposite relationship was true at the crown location impact, due to the increased contact area as shown in Figure 29. The 31A foam limited acceleration to approximately 130 *g* while the 51A foam showed acceleration over 200 *g*.

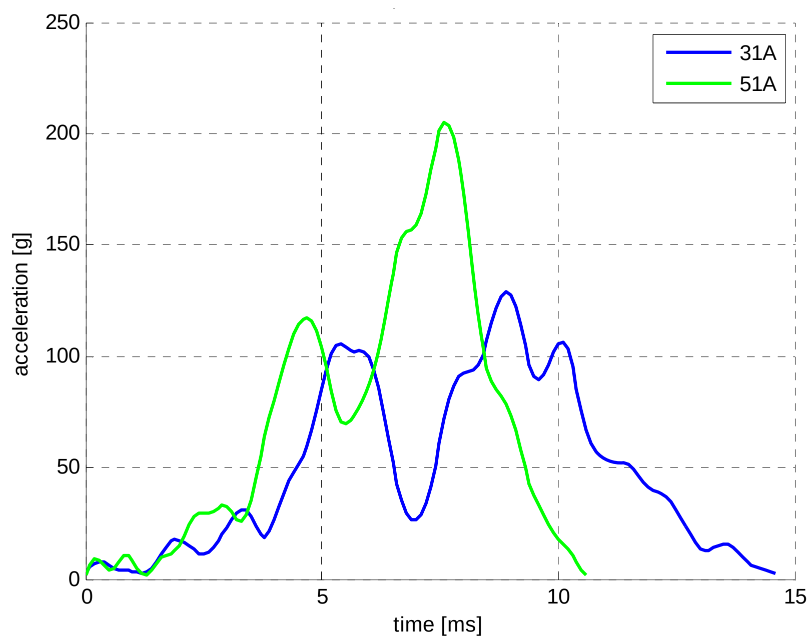

Figure 29. Crown location impact with ROHACELL® foam, 5.2 m/s (17 ft/s)

These test results were used to create a helmet liner prototype combining both densities of the ROHACELL® material. The addition of an extra 31A trapezoidal pad on the sides of the helmet was found to not significantly increase or decrease the resulting maximum acceleration of the side drops (when the other pads were all made of 51A). However, this added padding did result in more consistent data, as it prevented the occasional acceleration spikes caused by the headform impacting the side of the helmet. The pad configuration used in testing a ROHACELL® foam helmet liner prototype (shown in Figure 30) was one circular crown pad (31A), two trapezoidal side pads (31A), one front and one rear trapezoidal pad (51A), and four oblong pads located between front/back and side trap pads (51A).

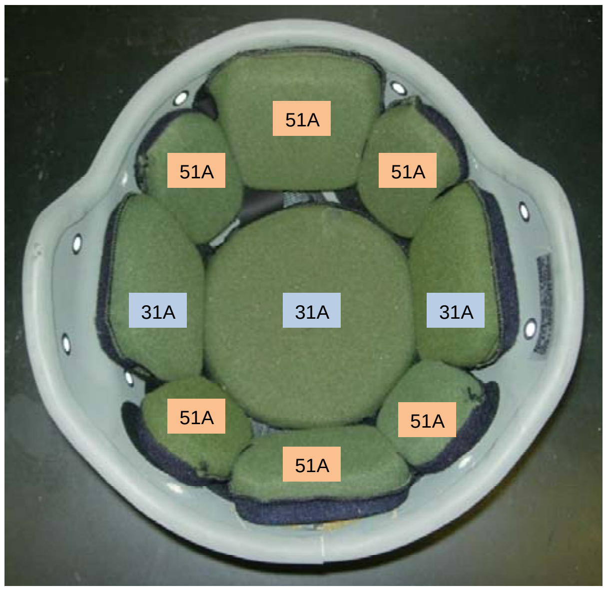

Figure 30. Configuration of ROHACELL® foam prototype

The test results for the ROHACELL® prototype at 5.2 m/s are shown in Table 7. Due to the crushing of the foam pads during impact, a second impact was not conducted, and the damaged foam was replaced after each impact.

Table 7. Test Results with 19 mm ROHACELL® Foam Prototype at 5.2 m/s (17 ft/s)

(Average of two tests)	
Impact Location	**Peak Acceleration (g)**
Rear	159
Front	144
Crown	132
Side	144
Nape	141

Although this material may not be practical in the field due to its crushable nature, it does demonstrate the effectiveness of this type of crushable foam as an impact energy absorber. The ROHACELL® prototype was able to pass the ACH required testing (two impacts at each location) at 3.0 m/s (10 ft/s); these results are presented in Appendix C.

4.3.2 Helmet Liner with Comfort Layer Prototype

PLASTAZOTE® HD80 is a material with a relatively high compression strength of 0.60 MPa. It absorbs energy through elastic and plastic deformation. Although it will lose some energy absorbing capacity after one impact, this material will remain intact and provide some protection for subsequent impacts. It is assumed that the HDPE foam will have a greater degree of temperature stability than the viscoelastic polyurethane foam used in the current ACH system. This was confirmed in testing of the helmet prototypes conditioned at 54 °C (130 °F).

The HD80 foam is die-cut and fixed in the ACH shell to create a partial helmet liner. The HDPE foams and crushable foams are rigid materials, and will require a comfort layer for application as a helmet liner. For this study, Poron® XRD™ polyurethane foam from Rogers Corporation was used for the comfort layer (17). The complete helmet prototype included 16 mm thick die-cut HD80 foam for impact absorption and 4 mm Poron XRD 09-158-65 for comfort and additional impact absorption.

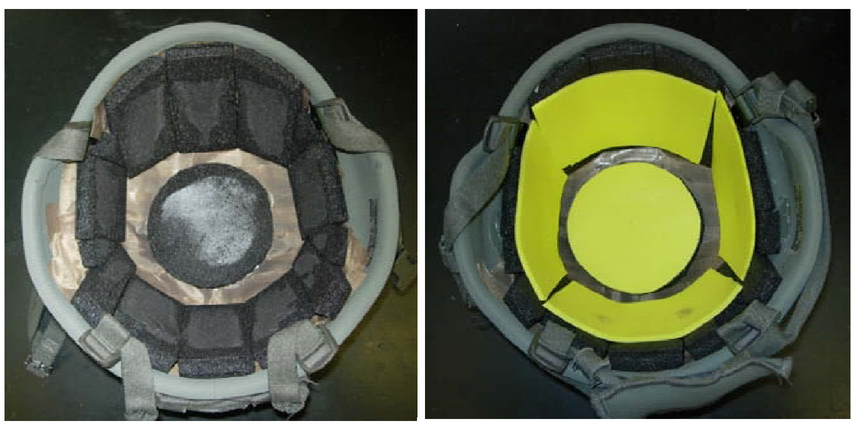

Figure 31. Plastazote® HD80 foam helmet liner with Poron® XRD™ comfort layer.

4.3.2.1 Test Results

The HD80 and Poron® XRD™ prototype was tested with two drops at all impact locations at 4.3 m/s and 5.2 m/s impact velocities in the ambient and hot conditions. The prototype test data was compared to the ACH system baseline data (15), which is the average of at least three test repetitions for each set of conditions. The NSRDEC prototype testing was the average of only two tests. The ambient temperature in the baseline testing was 22 °C, and the ambient temperature for the NSRDEC testing was between 24 and 26 °C. The sequence of the NSRDEC testing was back, front, crown, side, and nape. The nape impact often produces the highest peak acceleration, which may be due in part to the proximity between the nape and back impact locations.

The test results at 4.3 m/s for the HD80 prototype in the ambient and hot conditions are displayed in Table 8. The values for the side and nape conditions are the averages of the results from the right and left of each of those conditions. Any average peak accelerations exceeding the limit of 160 *g* are highlighted in red type. The HD80 prototype limited the average peak acceleration in the 4.3 ft/s impact test to 160 *g* in all but two of the test conditions.

Table 8. Current System and HD80/XRD, Ambient and Hot, Impact Velocity: 4.3 m/s (14 ft/s)

Impact Location	Current System				HD80/XRD			
	Ambient		Hot		Ambient		Hot	
	Drop 1	Drop 2	Drop 1	Drop 2	Drop 1	Drop 2	Drop 1	Drop 2
Rear	104	127	172	194	141	166	124	151
Front	171	178	163	162	121	144	110	132
Crown	111	116	108	109	139	154	119	143
Side	105	113	113	113	138	140	127	152
Nape	135	157	241	257	122	153	143	197

Peak acceleration in 14 ft./s. Impact: (>160 g highlighted in red)

The HD80 prototype test results at 5.2 m/s are displayed in Table 9. The values for the side and nape conditions are the averages of the results from the right and left of each of those conditions. At the higher impact velocity many of the peak acceleration results exceeded the 150 *g* limit. To assist in comparing the HD80 prototype to the current system, accelerations over 200 *g* are highlighted in red.

Table 9. Current System and HD80/XRD, Ambient and Hot, Impact Velocity: 5.2 m/s (17 ft/s)

Impact Location	Current System				HD80/XRD			
	Ambient		Hot		Ambient		Hot	
	Drop 1	Drop 2	Drop 1	Drop 2	Drop 1	Drop 2	Drop 1	Drop 2
Rear	170	338	471	492	171	257	230	484
Front	224	379	212	221	161	171	157	168
Crown	142	155	210	242	165	181	164	166
Side	163	348	191	194	157	198	221	282
Nape	300	510	492	489	201	329	436	629

Peak acceleration in 17ft./s. Impact: (>200 g highlighted in red)

Overall, the preliminary testing of the HD80 helmet prototype with Poron XRD comfort foam showed some improvement over the baseline data at 4.3 m/s. With some design improvements, this technology may have the potential to meet the 150 *g* acceleration limit for all ambient and hot conditions in a 4.3 m/s impact test. Samples of the acceleration vs. time data from the HD80/XRD prototype drop test experiments are presented in Appendix D.

Although the HD80 prototype did not perform up to the specifications at 5.2 m/s, it did limit the accelerations for the first drop in the ambient condition to approximately 200 *g* or less

4.3.2.2 Comparison with Model

The model of the partial foam liner with a comfort layer was compared to the HD80 prototype test results for the first drop of the ambient condition in a 5.2 m/s impact test, to determine If the model provided a sufficiently reasonable representation of the test results for use in future work to improve the design of the helmet liner. The side by side comparison of the prototype and model is displayed in Figure 32. The model was not created to perfectly match the geometry of the prototype, although the model and prototype are similar and were created with the same concept of a partial helmet liner created from foam sheet material.

Prototype | Finite Element Model

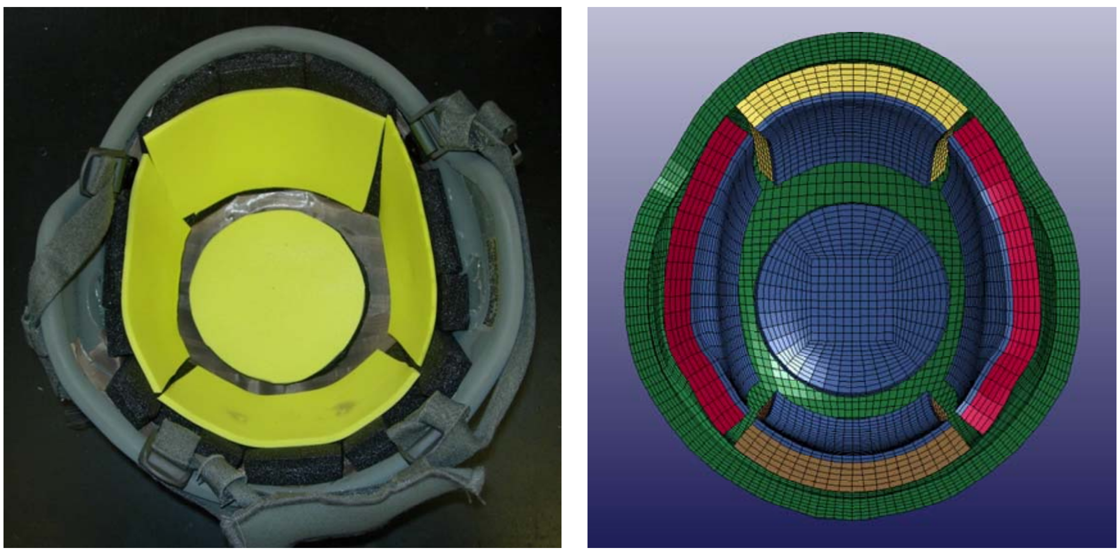

Figure 32. Helmet liner prototype and finite element model

Overlays of the experimental results and model simulation results are shown in Figure 33 for the front, back, crown, and side impact locations. The model provided an adequate prediction of the experimental results for the purposes of this study and can be used as a design tool in future efforts.

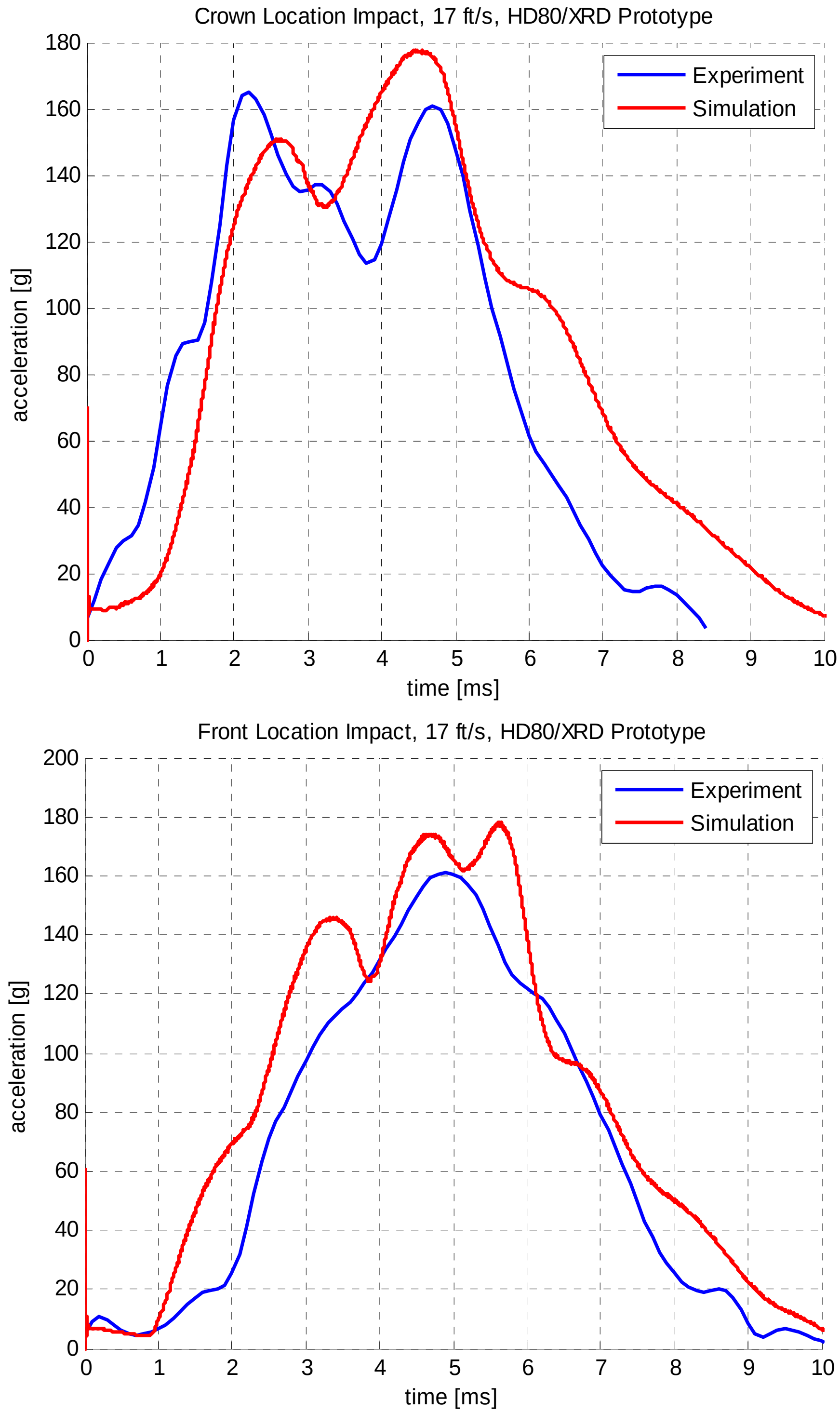

Figure 33. Comparison of experiment and model simulation of prototype at 5.2 m/s (17 ft/s)

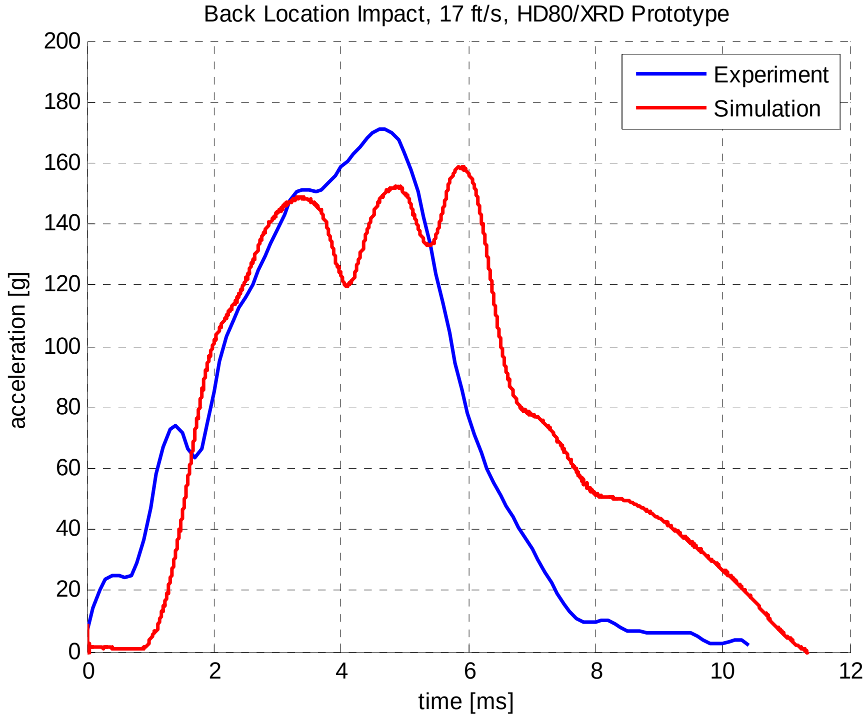

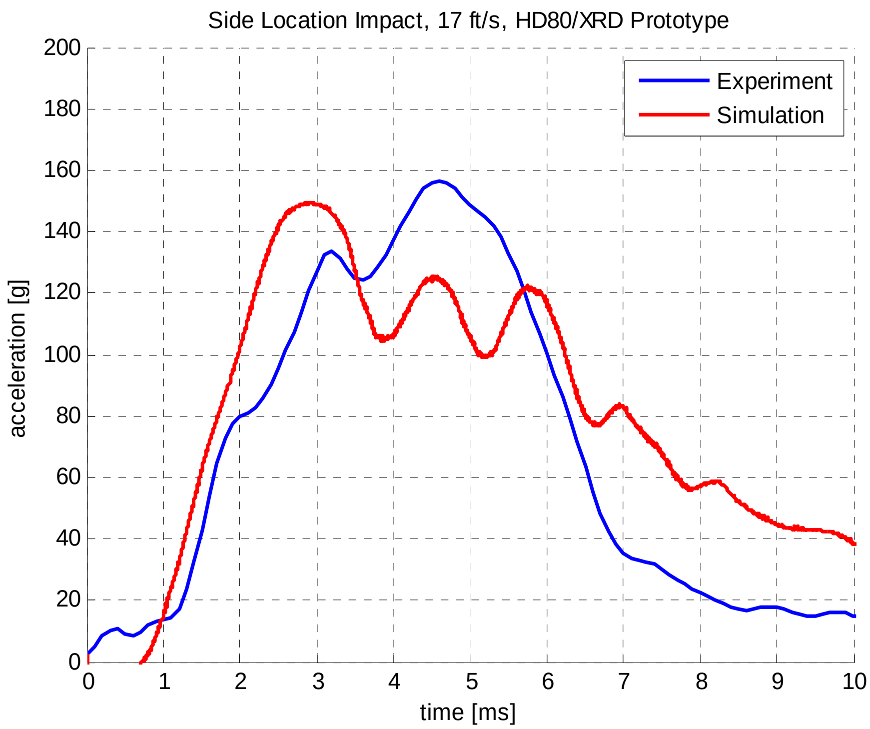

Figure 33. Comparison of experiment and model simulation of prototype at 5.2 m/s (17 ft/s) (Cont.)

The model results show a peak acceleration of approximately 150 *g* in the back and side locations, indicating the model was properly designed for these impacts. The front and crown locations show higher acceleration, indicating adjustments to the foam material could be made in those areas to improve the results and lower peak accelerations to 150 *g*.

5 Conclusions

5.1 *Summary*

The goal of this project was to design an improved energy absorbing helmet suspension system for low velocity impact protection, and to develop the material testing and computational modeling tools required to accomplish the task effectively. The basic concepts for packaging and energy absorbing helmet design were used as a starting point and combined with the impact test to identify potential materials for this application. A finite element model of the helmet, suspension system, and impact drop test was created to serve as a research tool in the design of an improved helmet suspension system. Helmet suspension system prototypes were designed and fabricated with two different types of materials. These prototypes were then tested in the helmeted headform drop test and compared with model predictions.

Crushable foam was demonstrated as an ideal material for a one time use application. A partial helmet liner of HDPE foam and a viscoelastic comfort layer was developed as a compromise of energy absorbing properties, durability (remaining intact after impact), and comfort. The experimental and model simulation results showed potential for this technology to meet the ACH test requirements at 4.3 m/s (14 ft/s) for the ambient and hot conditions.

The design of the helmet suspension system prototypes was based on using energy absorbing foam in a configuration similar to a helmet liner, which would increase the area coverage of material in the helmet. The specific fabrication techniques were used in part because foam materials are most readily available in sheet form, which can be cut to shapes and fixed inside the helmet. A final design could consist of a molded helmet liner, similar to a bicycle helmet shell. The specific materials used in this study were chosen based on a relatively limited search, and substitute materials with similar properties could likely produce similar results.

5.2 *Future Work*

The importance of material temperature stability is evident when testing helmets in the hot condition. Polymer foam materials will soften and lose strength at elevated temperatures. This issue also became evident when investigating differences in test results at different ambient temperatures. Testing materials over the range of operating temperatures and rates, including use of techniques such as dynamic mechanical analysis, should be included in future material testing.

Model simulations showed the response of the composite helmet shell could potentially have a significant effect on the acceleration trace of the headform. A simple isotropic material model was used to represent the helmet shell material. Improved modeling of the helmet shell material and structural response would lead to improved accuracy of the model simulations. This must include the ability to predict the composite material damage on impact with the anvil, which affects the energy absorption of the helmet.

This document reports research undertaken at the U.S. Army Natick Soldier Research, Development and Engineering Center, Natick, MA, and has been assigned No. NATICK/TR- 13/016 in a series of reports approved for publication.

6 References

1. **Team Wendy.** Team Wendy Materials. [Online] [Cited: September 27, 2012.] http://www.teamwendy.com/technology/materials/.

2. **Granta Material Intelligence.** Materials for Bicycle Helmets. [Online] [Cited: 6 23, 2010.] www.grantadesign.com/resources/materials/casestudies/helmet.

3. **Gibson, L.J.** *Cellular Solids: Structure and Properties- Second edition.* Cambridge, UK : Cambridge University Press, 1997.

4. *Bicycle Helmet Design.* **Mills, N.J.** 2006, Journal of Materials, Design and Applications, pp. 220(L4): pp. 167-180.

5. **Program Executve Office - Soldier.** *Purchase Description, Helmet, Advanced Combat (ACH) CO/PD-05-04.* Fort Belvoir, VA : Technical Management Division, PM Soldier Equipment, 2007.

6. **Livermore Software Technology Corporation.** *LS-Dyna Keyword User's Manual, Version 971.* 2007. pp. 226-227, 314.

7. **Evonik Rohm GmbH.** Rohacell-A: Aircraft Grade. [Online] January 2011. [Cited: September 27, 2012.] http://www.rohacell.com/product/rohacell/en/products-services/rohacell-a/pages/default.aspx.

8. **Quality Foam Packaging.** Quality Foam - Zotefoams Plastazote. [Online] January 2004. [Cited: September 27, 2012.] http://www.qualityfoam.com/plastazote.

9. **Corner, Brian.** 3D scans of ACH and DOT-C headform. s.l. : NSRDEC Anthropology Team, 2012.

10. **Department of the Army.** *Technical Operator's Manual for Advanced Combat Helmet (ACH) TM 10-8470-204-10.* Washington, DC : Headquarters, Department of the Army, 2008.

11. **Moss, W.C.** *Impact Response of US Army and National Footbal League Helmet Pad Systems.* Livermore, CA : Lawrence Livermore National Laboratory, 2011.

12. *Numerical Head and Composite Helmet Models to Predict Blunt Trauma.* **Van Hoof, J.** 2001 : s.n., 2001. 19th International Symposium of Ballistics. pp. 921-928.

13. **U.S. Department of Transportation.** *Laboratory Test Procedure for Motorcycle Helmets, FMVSS 218.* Washington, DC : National Highway Traffic Safety Administraion, Office of Vehicle Safety Compliance, 2006.

14. **Cunniff, Philip.** Technical Plan: Low Velocity Impact Protection System. s.l. : NSRDEC Ballistics Team, 2011.

15. **Technical Management Division (TMD), Project Manager Soldier Protection and Individual Protection (PM-SPIE).** Helmet/Headform Low Velocity Impact Test Data, Phase 2A. Haymarket, VA : s.n., 2010.

16. *Methodologies for Blunt Trauma Assessment in Military Helmets.* **Hopping, J.** Quebec City : s.n., 2010. Personal Armour Systems Symposium.

17. **Rogers Corporation.** Poron XRD Extreme Impact Protection. [Online] 2010. [Cited: September 28, 2012.] http://www.poronxrd.com/.

This page intentionally left blank

Appendix A

LS-Dyna® Model Materials, Definitions, and Conditions

Table A-1. Consistent Units in Model

Mass	ton
Length	mm
Time	s
Force	N
Stress	MPa
Energy	N-mm

Table A-2. Materials

Magnesium Headform		
*MAT_RIGID		
ro	e	pr
1.64E-09	42000	0.3

Steel Anvil		
*MAT_RIGID		
ro	e	pr
7.89E-09	2.10E+05	0.3

Helmet - isotropic model						
*MAT_ISOTROPIC_ELASTIC_PLASTIC						
ro	g	sigy	etan	bulk		
1.23E-09	7400	77	0	12330		
Helmet - orthotropic model						
*MAT_COMPOSITE_DAMAGE						
ro	ea	eb	ec	prba	prca	prcb
1.23E-09	18500	18500	6000	0.25	0.25	0.25
gab	gbc	gca	kfail	aopt	macf	
770	2720	2720	100	1	3	

Helmet Retention Spring
*MAT_SPRING_NONLINEAR_ELASTIC
spring constant in tension: 500 N/mm
spring constant in compression: 0 N/mm

Table A-3. Crushable Foam Pads

*MAT_CRUSHABLE_FOAM					
	ro	e	pr	tsc	damp
31A	3.0E-11	10.0	0.01	1.00E+10	0.01
51A	5.0E-11	10.0	0.01	1.00E+10	0.01

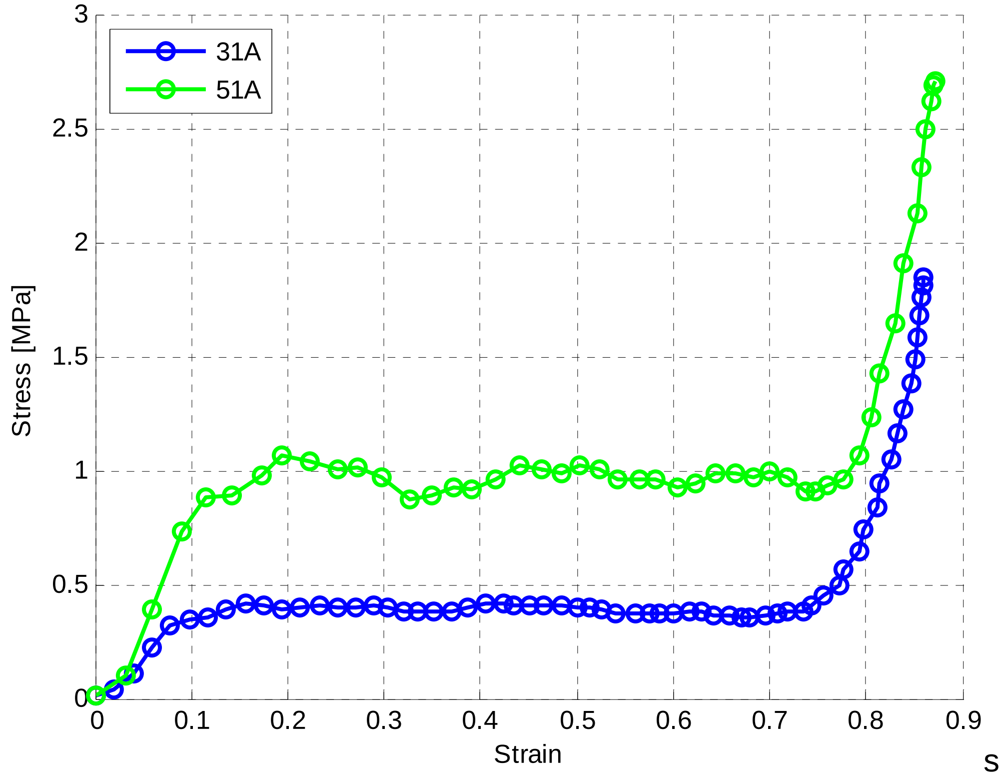

Figure A-1. Stress vs. strain for input to LS-DYNA crushable foam model (MAT63)

Table A-4. Low Density Foam Pads

*MAT_LOW_DENSITY_FOAM						
	ro	e	tc	hu	damp	shape
ACH Pad	1.0E-10	1.00	1.00E+10	0.25	0.10	5.00
HD80	8.0E-11	1.00	1.00E+10	0.2	0.10	4.00
XRD	1.4E-10	1.00	1.00E+10	0.2	0.10	3.00

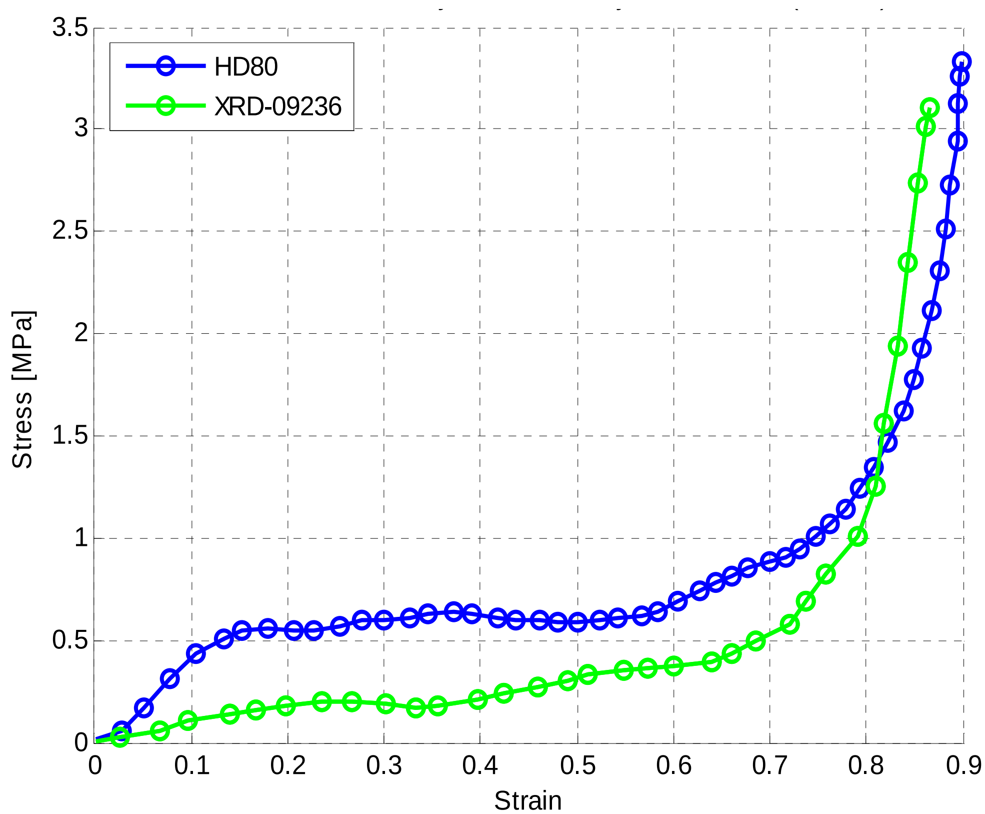

Figure A-2. Stress vs. strain for input to LS-DYNA low density foam model (MAT57)

Table A-5. Contact Definitions

Contact between headform and foam pads defined by part IDs *CONTACT_AUTOMATIC_ONE_WAY_SURFACE_TO_SURFACE
Interface between foam pads and helmet inner surface (If foam pads are pressed into helmet surface) *CONTACT_CONSTRAINT_SURFACE_TO_SURFACE
Tied interface between foam pads and helmet inner surface (If foam pads are projected into helmet surface) *CONTACT_TIED_NODES_TO_SURFACE
Contact between all other foam pad nodes and helmet inner surface *CONTACT_AUTOMATIC_NODES_TO_SURFACE
Contact between helmet and anvil defined by part IDs *CONTACT_AUTOMATIC_SURFACE_TO_SURFACE
Contact between headform and helmet inner surface *CONTACT_AUTOMATIC_SURFACE_TO_SURFACE

Table A-6. Initial Conditions and Boundary Conditions

Boundary Conditions during fitting stage Prescribed motion to insert headform in to helmet *BOUNDARY_PRESCRIBED_MOTION_RIGID Back surface nodes of foam pads are constrained *BOUNDARY_SPC_SET **Full Restart** Simulation restart when headform is in position *STRESS_INITIALIZATION Spring is added to retain helmet on headform *ELEMENT_DISCRETE **Boundary Conditions during impact stage** Intial velocity of headform and helmet *CHANGE_VELOCITY_RIGID_BODY *CHANGE_VELOCITY Headform is constrained from horizontal motion *BOUNDARY_PRESCRIBED_MOTION_RIGID

Appendix B

Test Results and Model Simulation of ROHACELL® Foam Prototypes

Figure B-1. Test results and model simulation of ROHACELL®-31A foam prototype, 5.2 m/s (17 ft/s)

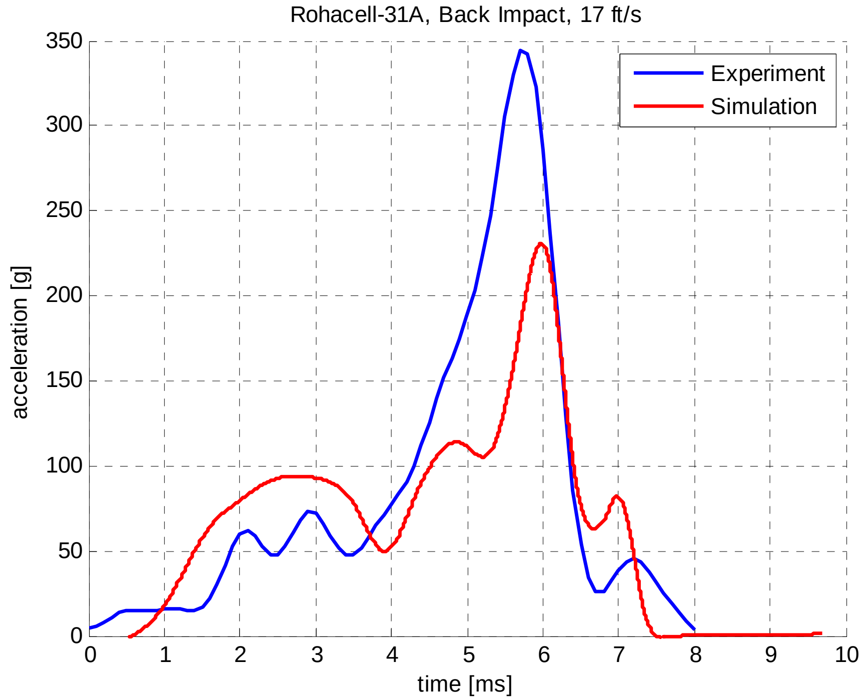

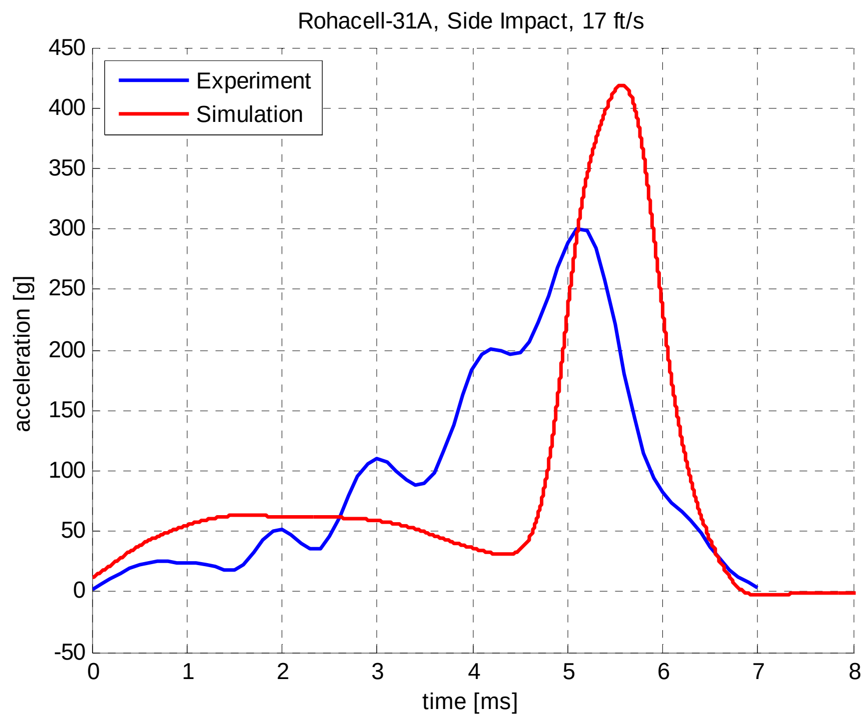

Figure B-1. Test results and model simulation of ROHACELL®-31A foam prototype, 5.2 m/s (17 ft/s) (Cont.)

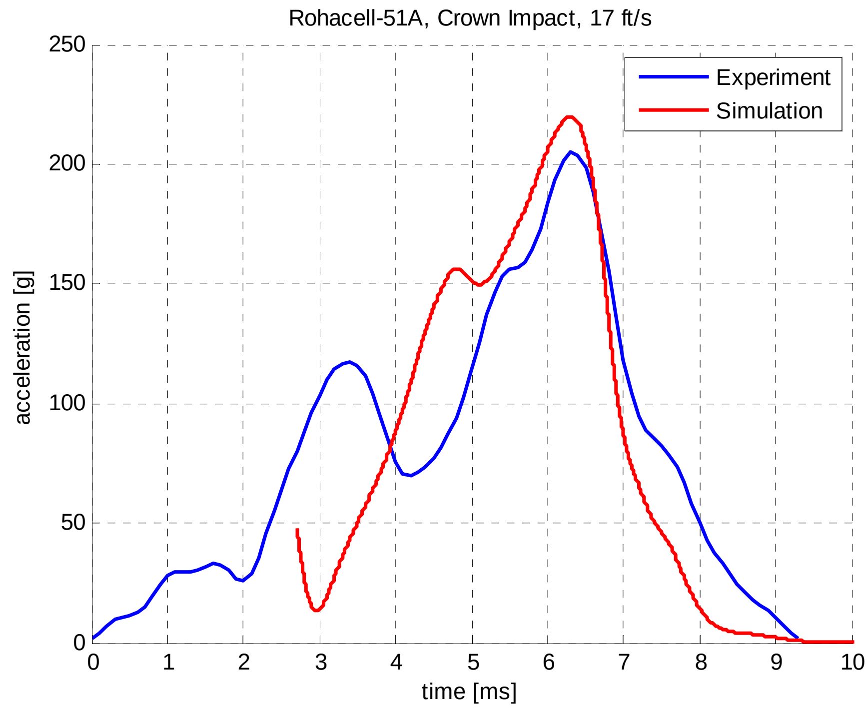

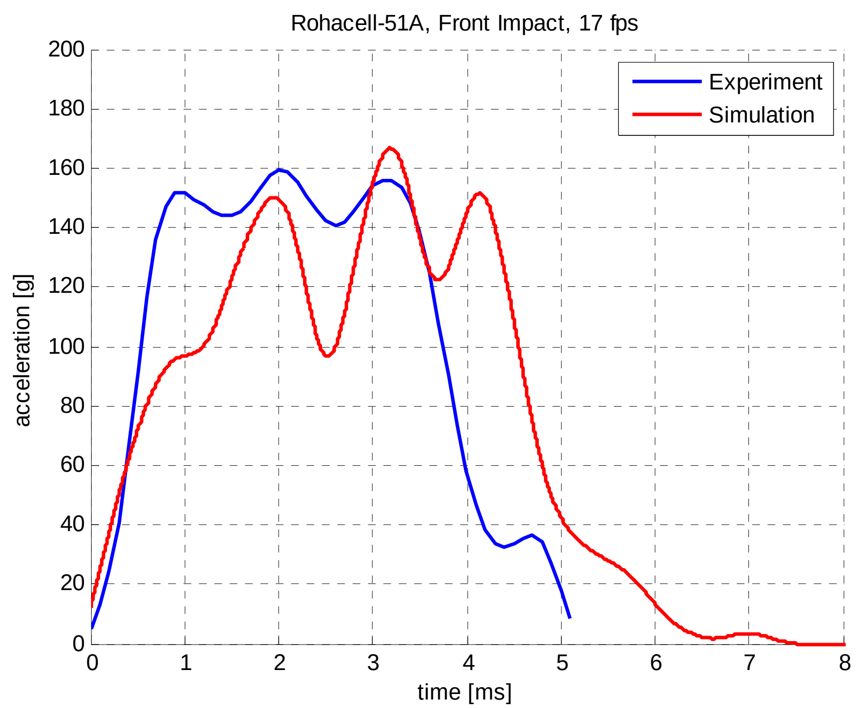

Figure B-2. test results and model simulation of ROHACELL®-51A foam prototype, 5.2 m/s (17 ft/s)

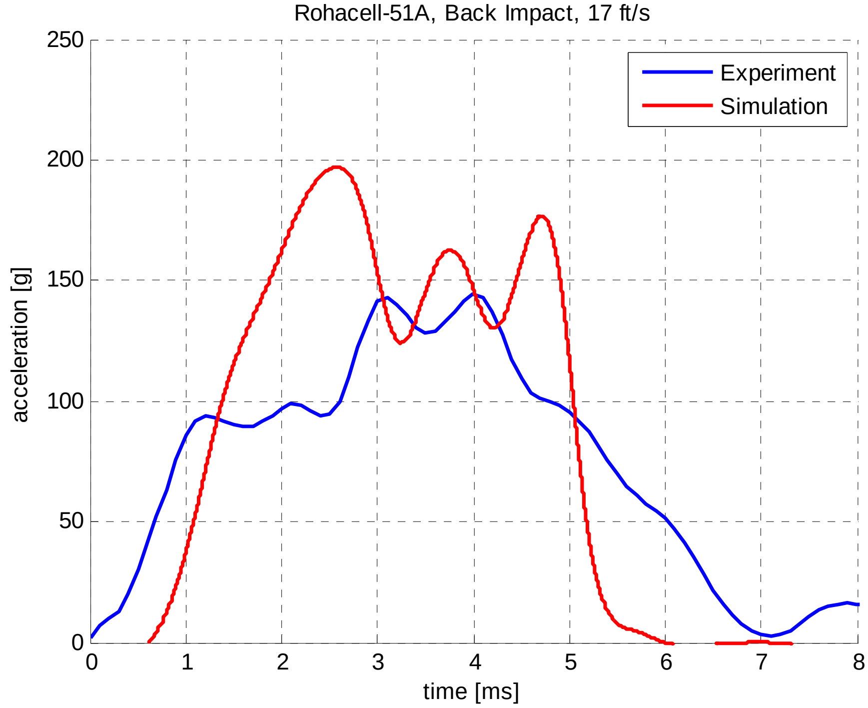

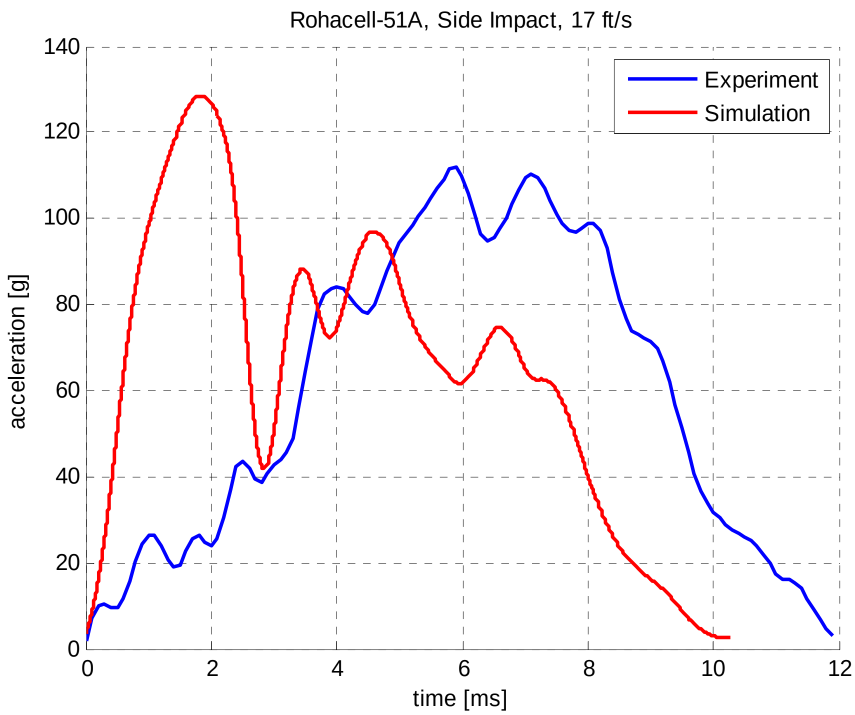

Figure B-2. Test results and model simulation of ROHACELL® -51A foam prototype, 5.2 m/s (17 ft/s) (Cont.)

Appendix C

Results of Helmet Drop Tests with 19mm ROHACELL® Foam Padding System at 3 m/s (10 ft/s)

Impact Location		Peak Acceleration (*g*/s)			
		ROHACELL Prototype		Team Wendy system (avg)	
		Drop 1	Drop 2	Drop 1	Drop 2
Rear		100.7	127.2	72.1	76.4
Front		65.2	104.5	123.9	140.4
Crown		135.5	101.3	76.7	79.2
Side	Left	111.1	142.5	73.5	81.9
	Right	94.4	152.3	65.9	73.2
Nape	Left	101.9	127	67.7	73.7
	Right	73.3	115.8	69.6	80.7

This page intentionally left blank

Appendix D

Samples of the Acceleration vs. Time Data from the HD80/XRD Prototype Drop Test Experiments

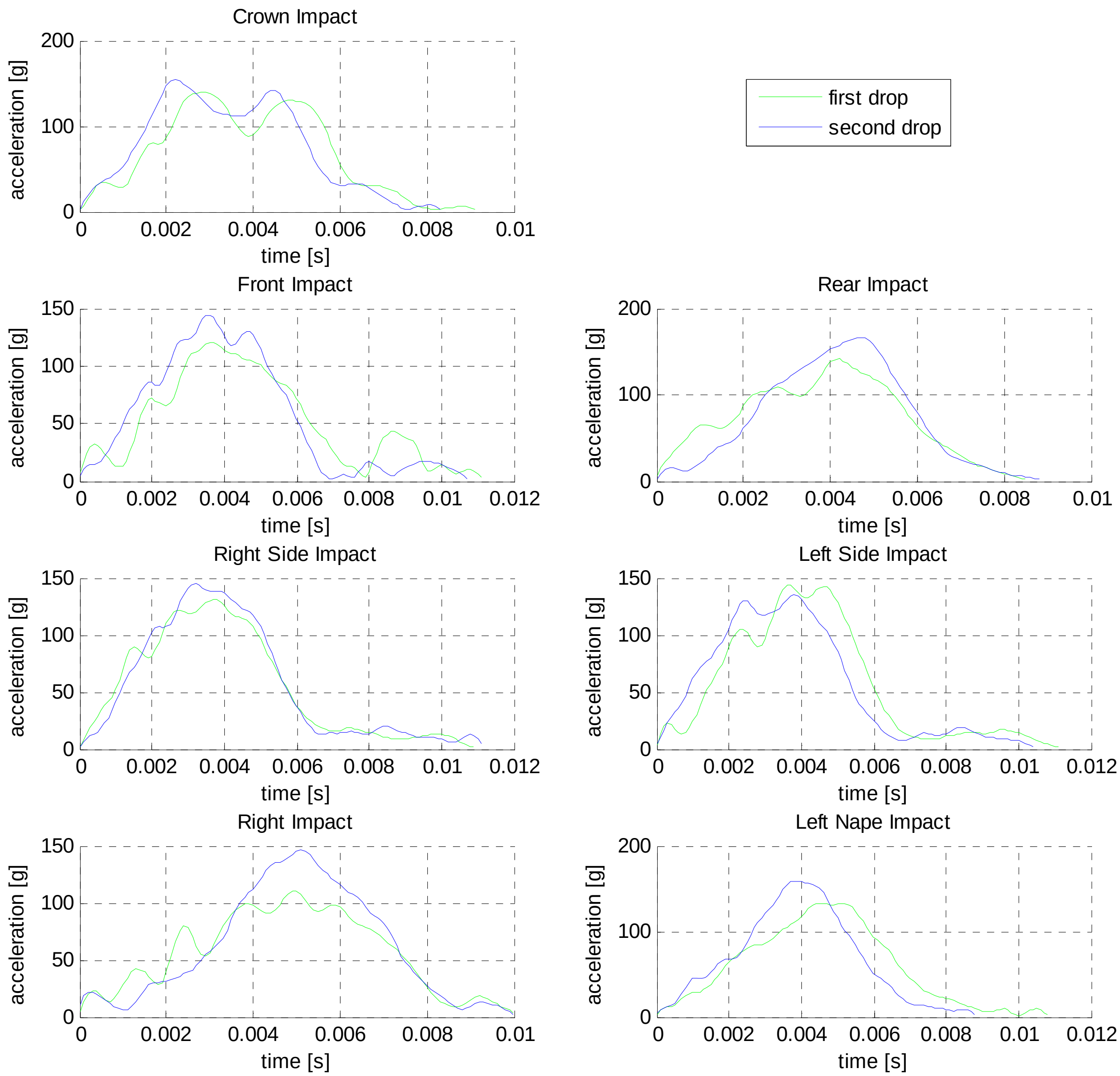

Figure D-1. HD80 prototype with comfort layer– ambient temperature condition, 4.3 m/s (14 ft/s)

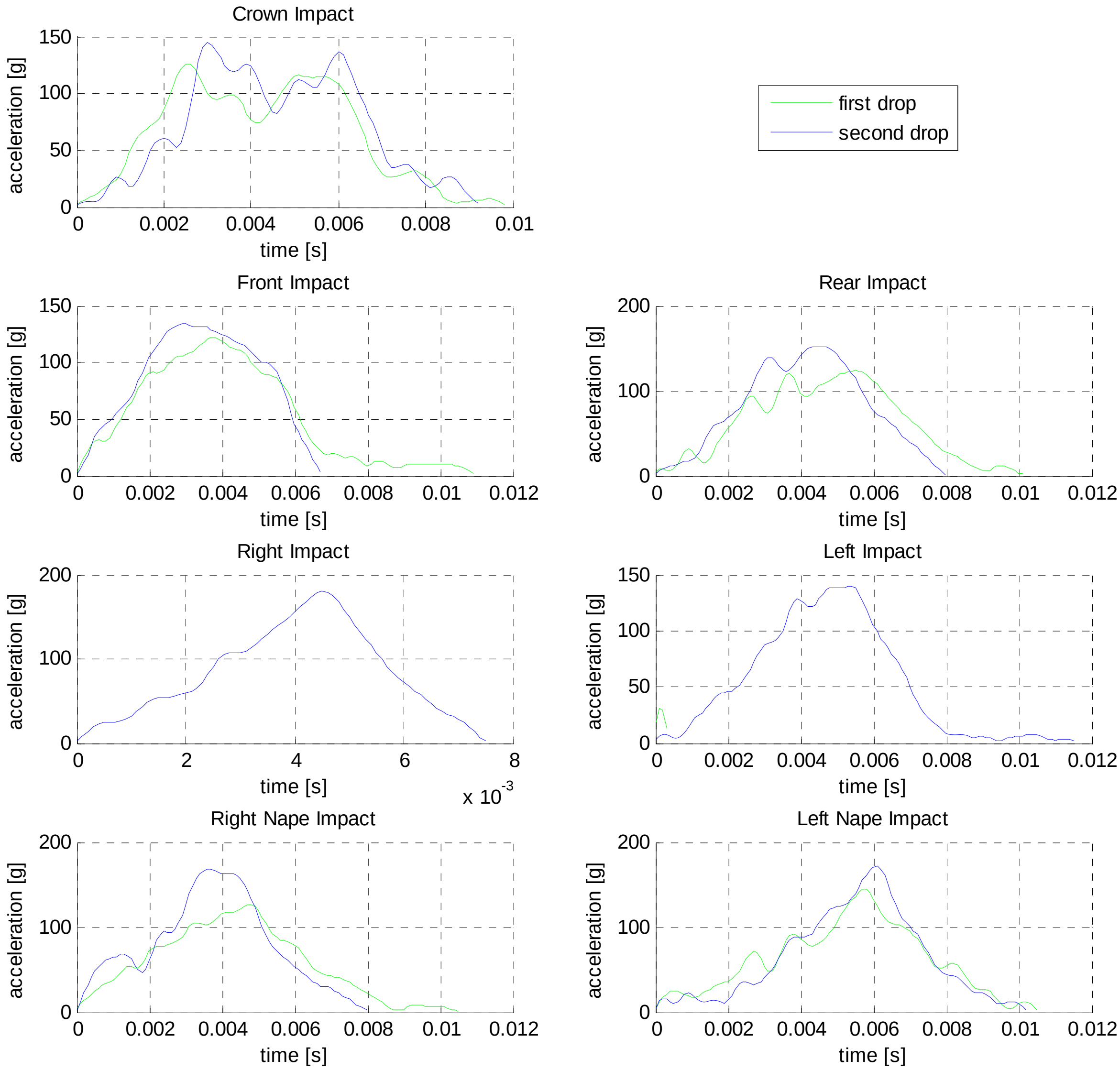

Figure D-2. HD80 prototype with comfort layer – hot (54 °c) temperature condition, 4.3 m/s (14 ft/s)

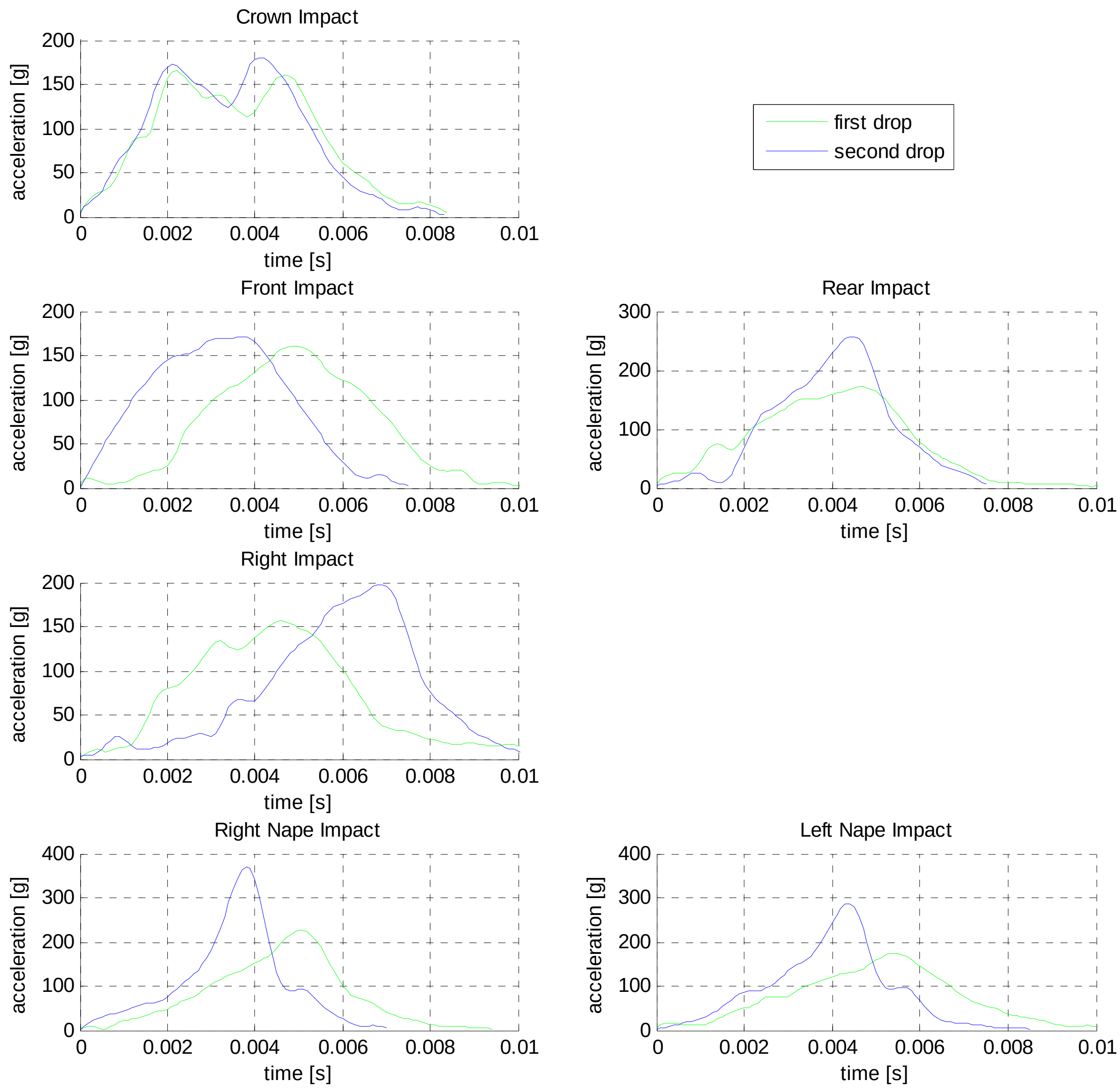

Figure D-3. HD80 prototype with comfort layer – ambient temperature condition, 5.2 m/s (17 ft/s)

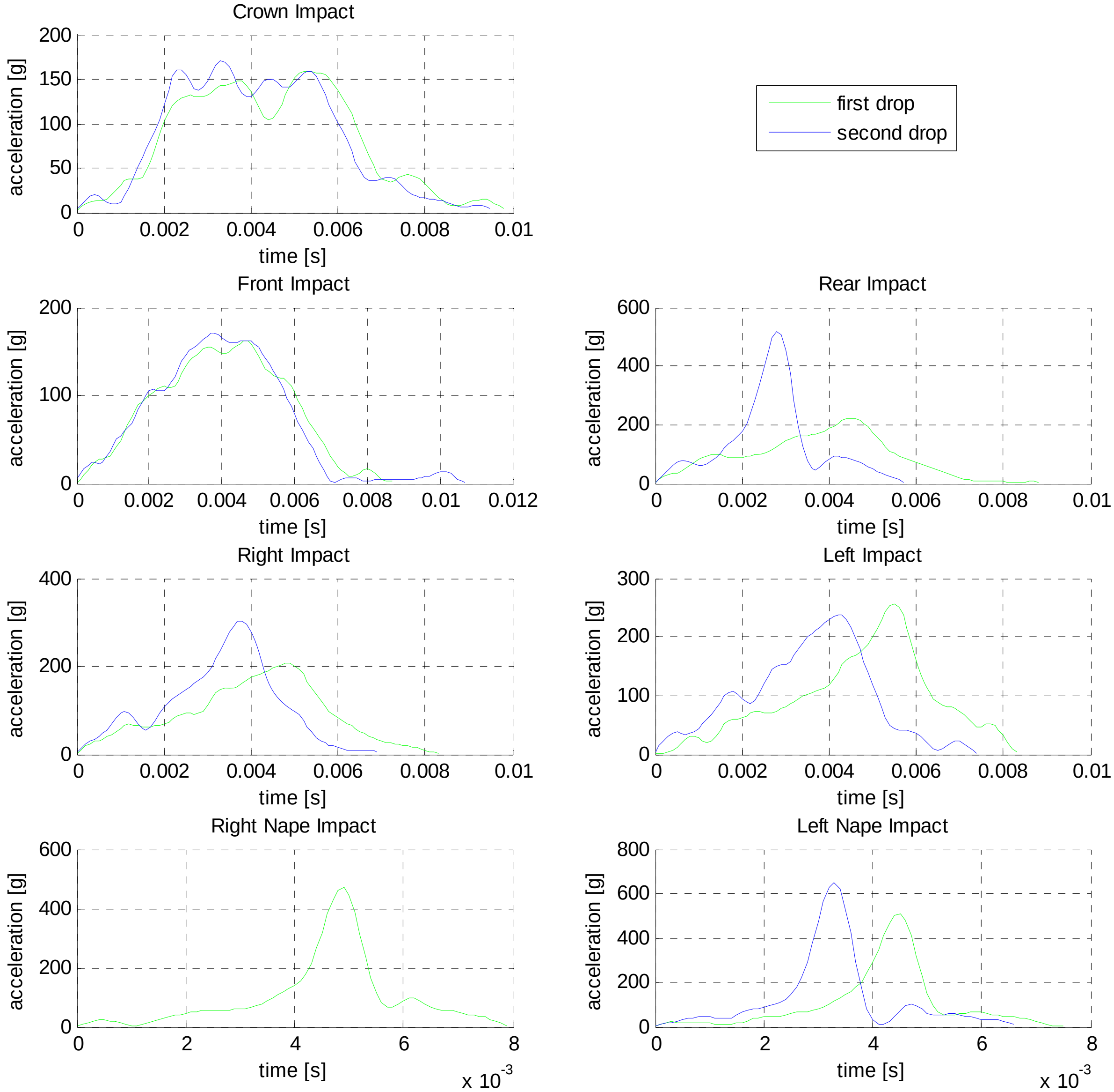

Figure D-4. HD80 prototype with comfort layer – hot (54 °c) temperature condition, 5.2 m/s (17 ft/s)